EFFECT OF RADIATION ON FREE CONVECTION FLOW ON A SPHERE WITH ISOTHERMAL SURFACE AND UNIFORM SURFACE HEAT FLUX

by

TAHMINA AKHTER
Student No. 100009007
Registration No. 0010247, Session: October-2000

MASTER OF PHILOSOPHY
IN
MATHEMATICS

Department of Mathematics
BANGLADESH UNIVERSITY OF ENGINEERING AND TECHNOLOGY, DHAKA-1000
April- 2007

The thesis titled

Effect of Radiation on Free Convection Flow on a Sphere With Isothermal Surface and Uniform Surface Heat flux.

Submitted by

TAHMINA AKHTER

Student No. 100009007, Registration No. 0010247, Session: October-2000, a part time student of M. Phil. (Mathematics) has been accepted as satisfactory in partial fulfillment for the degree of

Master of Philosophy in Mathematics

17th April- 2007

BOARD OF EXAMINERS

1. A. Alim

Dr. Md. Abdul Alim
Assistant Professor
Dept. of Mathematics, BUET, Dhaka-1000

Chairman (Supervisor)

2. Manirul A Sarker

Dr. Md. Manirul Alam Sarker
Associate Professor
Dept. of Mathematics, BUET, Dhaka-1000

Member

3. MChowdhury

Dr. Md. Mustafa Kamal Chowdhury
Professor and Head
Dept. of Mathematics, BUET, Dhaka-1000

Member (Ex-Officio)

4. [signature]

Dr. Md. Arif Hasan Mamun
Assistant Professor
Dept. of Mechanical Engineering
BUET, Dhaka-1000

Member (External)

Abstract

In this thesis, the effects of radiation on free convection flow with isothermal surface and with uniform surface heat flux on a sphere have been investigated. The physical problems are represented mathematically by different sets of governing equations along with the corresponding boundary conditions. Using appropriate transformations, the governing equations containing equations of continuity, momentum and energy are transformed into a set of non-dimensional boundary layer equations subject to appropriate boundary conditions, which are then solved numerically with the Keller box scheme of finite-difference method.

Here importance has been given on the evaluation of surface shear stress in terms of local skin friction. rate of heat transfer in terms of Nusselt number also on velocity profiles as well as temperature profiles. A selected parameter set is also considered for computation consisting of radiation parameter Rd, surface temperature parameter θ_w and Prandtl number Pr. The results in terms of local skin friction, local Nusselt number are shown in tabular forms. Velocity profiles, temperature profiles, skin friction coefficient and rate of heat transfer have been displayed graphically for various values of radiation parameter, surface temperature parameter separately and the Prandtl number as well.

Author's Declaration

I am hereby declaring that the work in this dissertation was being carried out in accordance with the regulations of Bangladesh University of Engineering and Technology (BUET), Dhaka, Bangladesh .The work is also original except where indicated by and attached with special reference in the context and no part of it has been submitted for any attempt to get other degrees or diplomas.

All views expressed in the dissertation are those of the author and in no way or by no means represent those of Bangladesh University of Engineering and Technology, Dhaka. This dissertation has not been submitted to any other University for examination either in home or abroad.

(Tahmina Akhter)

Date: 17th April 2007

Acknowledgements

To my great delight. I would like to have the opportunity to express my heart-rending appreciation and profound sense of gratitude to my Supervisor Dr. Md. Abdul Alim, Assistant Professor, Department of Mathematics, who has encouraged and rightly initiated me to step into the wide arena of Mathematics and its application in the engineering fields.

I am no less grateful and thankful to the efforts, perseverance, sincerity, enormous will force, clarity, accuracy, completeness, monumental patience, generous co-operation and fellow-feeling he made for me to venture this research and bring this painstaking task to a successful end.

I am also deeply indebted to Prof. Dr. Md. Mustafa Kamal Chowdhury, Head of the Department of Mathematics. BUET and Dr. Manirul Alam Sarker, Associate Professor Department of Mathematics BUET, Dhaka-1000 for their wise and liberal co-operation in providing me of all necessary help from the department during my course of M.Phil degree.

I would also like to extend my thanks to all other teachers and other concerned with this department for their help and co-operation. It is also a subject of joy for me to thank Ms. Minufar Choudhury, professor and coordinator of the Inter departmental courses and all of my colleagues of The University of Asia Pacific for their visionary encouragement to complete the M.Phil degree.

It is with particular pleasure to express my gratefulness to Md. Mahmud Alam, Assistant Professor, Department of Mathematics, DUET, Gazipur, for his inspiration and unhindered co-operation to bring this venture to a meaningful conclusion. Finally, I must acknowledge my debt to my parents for whom I have been able to see the beautiful sights and sounds of the world. Last but not the least, it would be ungrateful for me if I do not evaluate the efforts and pains taken by my husband during the struggle-some course.

Contents

Nomenclature

a	Radius of the sphere [m]
C_f	Local skin friction coefficient [-]
C_p	The specific heat due to constant pressure [$kJkg^{-1}k^{-1}$]
f	Dimensionless stream function [-]
f'	Derivative of f with respect to η [-]
Gr	Grashof number [-]
g	Acceleration due to gravity [ms^{-2}]
Nu	Local Nusselt number [-]
Pr	Prandtl number [-]
q_r	Radative heat flux [w/m^2]
q_c	Conduction heat flux [w/m^2].
Rd	Radiation parameter [-]
r	Radial distance from the symmetric axis to the surface [m]
T	Temperature of the fluid in the boundary layer [T]
T_∞	Temperature of the ambient fluid [T]
T_w	Temperature at the surface [T]
$(\underline{u}, \underline{v})$	Velocity components along the (x, y) axis [ms^{-1}]
(u, v)	Dimensionless velocity components along the (x, y) axis [-]

Greek symbols

α_r	Rosseland mean absorption co-efficient [cm^3/s]
β	Coefficient of thermal expansion [k^{-1}]
θ	Dimensionless temperature function [-]
θ_w	Surface temperature parameter [-]
κ	Thermal conductivity [$wm^{-1}k^{-1}$]
μ	Viscosity of the fluid [m^2/s]
ν	Kinematic viscosity [m^2s^{-1}]
ρ	Density of the fluid [kgm^{-3}]
σ	Electrical conductivity [$mho.m^{-1}$]
σ_s	Scattering co-efficient [lm]
τ_w	Wall shear stress [$dynes/cm^2$]
ψ	Stream function [m^2s^{-1}]
(ξ, η)	Dimensionless coordinate along the (u, v) axis [-]

List of Tables

List of Figures

Chapter 1

1.1 Introduction

Radiation is transformed in the form of ectromagnetic waves that directly transport energy through space and this is the only process, which brings light and heat to our planet, earth from the sun, which is millions of miles away from us. Convection is the transfer of heat by the actual movement of the warmed matter. It cannot occur in solids due to the particles not being able to flow freely. The most common cause of internal movement is a variation in density due to transfer of heat. Free convection is the convection in which motion of the fluid arises solely due to the density gradients (for example, due to temperature differences existing within the fluid) that can be maintained in the fluid, for example hot air rising off the surface of a radiator.

A body is introduced into a fluid at different temperatures forms a source of disturbance due to the thermal interaction between the body and the fluid. The fluid elements near the body surface assume the temperature of the body and then begin the propagation of heat into the fluid and the variation of temperature is accompanied by density variations. In particular, if the density variation is caused by the non-uniformity of the temperature it is called convection. The convective mode of heat transfer is generally divided into two basic processes. If the motion of the fluid arises from an external agent then the process is termed forced convection. This type of fluid flow is caused in general by a fan, blower, the bursting of a tire etc. Such problems are very frequently encountered in technology where the heat transfers to or from a body is often due to imposed flow of a fluid of different temperature from that of the body. On the other hand, if no such externally induced flow is provided and the flow arises from the effect of a density difference resulting from temperature or concentration difference. in a body forced field such as the gravitational field, then the process is termed natural convection. Generally, the density difference gives rise to buoyancy forces, which drive the flow. Buoyancy induced convective flow is of great importance in many heat removal processes in engineering technology and has attracted the attention of many researchers in the last few decades due to the fact that both science and technology are being interested in passive energy storage systems, such as the cooling of spent fuel rods in nuclear power applications and the design of solar collectors. In particular, it has been ascertained that free convection induced the thermal stress, which leads to critical structural damage in the piping systems of nuclear reactors. The buoyant flow arising from heat rejection to the atmosphere. heating of rooms, fires. and many other heat transfer processes. are other examples of natural convection flows.

The effects of radiation on free convection flow are important in the context of space technology and very little is known about the effects of radiation on the boundary layer flow of a radiating fluid past a body. The inclusion of a radiation effects in the energy equation, however, leads to a highly non-linear partial differential equation. The problem of free convection boundary layer over or on various shapes such as vertical flat plate, cylinder, sphere, etc, have been studied by many investigators and it has been a very popular research topic for many years. It is readily recognized that a wealth of information is now available on convective heat and mass transfer for viscous (Newtonian) fluids

The study of temperature field and heat transfer is of great importance to the engineers because of its almost universal occurrence in many branches of science and engineering. Although heat transfer analysis is most important for the proper sizing of fuel elements in the nuclear reactors cores to prevent burnout. The performance of aircraft also depends upon the case with which the structure and engines can be cooled. The design of chemical plants is usually done on the basis of heat transfer analysis and the analogous mass transfer processes. The amount of energy transfer as heat can be determined from energy-conservation consideration (first law of thermodynamics). Energy transfer as heat will take place from the assembly (body) with the higher temperature, if these two are permitted to interact through a diathermal wall (second law of thermodynamics). The transfer and conversion of energy from one form to another is the basis to all heat transfers processes and hence, the first as well as the second law of thermodynamics govern them. Heat transfer is commonly associated with fluid dynamic. The knowledge of temperature distribution is essential in heat transfer studies because of the fact that the heat flow takes place only wherever there is a temperature gradient in a system. The heat flux which is defined as the amount of heat transfer per unit area per unit time can be calculated from the physical laws relating to the temperature gradient.

Numerous industrial applications involve both forced and natural convection along ax symmetric bodies where special effects such as body rotation, surface mass transfer, the heating/cooling mode, and the type of thermal wall condition are important. Examples include rotary machine design, transportation cooling, projectile behavior, and wire and fiber coating. Spin motion enhances convection heat transfer when the centrifugal force pushes the near surface fluid outward, which is being replaced by cooler or warmer fluid depending upon the wall temperature.

Nazar et al. (2002a, 2002b) considered the free convection boundary layer flow on an isothermal horizontal circular cylinder and on an isothermal sphere for micro polar fluid. Yao (1983) has studied the problem of natural convection flow along a vertical wavy surface. Also the problem of free convection boundary layer on a vertical plate with prescribed surface heat flux investigated by Merkin and Mahmood (1990).

The governing partial differential equations are to deal with in the case of incompressible viscous fluid such as continuity equation, momentum equation and energy equation. The radiation energy emitted by a body is transmitted in the space in the form of electromagnetic waves according to Maxwell's classic electromagnetic wave theory or in the form of discrete photons according to Planck's hypothesis. Both concepts have been utilized in the investigation of radiative-heat transfer. The emission or absorption of radiation energy by a body is a bulk process; that is, radiation originating from the interior of the body is emitted through the surface. Conversely, radiation incident on the surface of a body penetrates to the depths of the medium where it is attenuated. When a large proportion of the incident radiation is attenuated within a very short distance from the surface, we may speak of radiation as being absorbed or emitted by the surface. For example, thermal radiation incident on a metal surface is attenuated within a distance of a few angstroms, from the surface: hence metals are opaque to thermal radiation.

Many mathematicians, versed engineers and researchers have studied the problems of free convection boundary layer flow over or on a various types of shapes. Amongst them are Hossain and Takhar (1996), Huang and Chen (1987), Merkin and Mahmood (1990), Nazar et al (2002a, 2002b) and Molla et al (2005). Huang and Chen (1987), Nazar et al (2002a, 2002b) considered the free convection boundary layer on an isothermal sphere and on an isothermal horizontal circular cylinder both in a micro polar fluid. Molla et al (2004) have studied the problem of natural convection flow along a vertical wavy surface with uniform surface temperature in presence of heat generation or absorption. The problem of the free convection boundary layer on a vertical plate with prescribed surface heat flux was studied by Merkin and Mahmood (1990). Also the effects of axial heat conduction in a vertical plate on free convection heat transfer have been studied by Miyamoto et al. (1980). On the other hand, the coupling of conduction with laminar natural convection boundary layer flow along a flat plate was investigated by Pozzi and Lupo (1988).

A transformation of the boundary layer equations for natural convection flow past a vertical plate with an arbitrary blowing and wall temperature variations was studied by Vedhanayagam et al. (1980). The case of a heated isothermal horizontal surface with transpiration was discussed in some detail first by Clarke and Riley ((1975, 1976), and then by Lin and Yu (1988). Hossain and Takhar (1996) also discussed the same problems but with the temperature dependent viscosity and thermal conductivity. Soundalgekar et al. (1960) have studied radiation effects on free convection flow of a gas past a semi-infinite flat plate using the Cogley-Vincenti-Giles equilibrium model Cogley et al(1968), later Hossain and Takhar (1996) have analyzed the effects of radiation using the Rosseland diffusion approximation which leads to non-similar solutions for free convection flow past a heated vertical plate. Limitations of this approximation are discussed briefly in Özisik (1973). The above investigators were not concern about the uniform heat flux. But in our present study we have investigated these criteria by using necessary boundary conditions.

In present work, the effects of radiation on free convection flow around a sphere with isothermal surface and uniform heat flux have been investigated. The results are obtained for different values of relevant physical parameters. The natural convection boundary layer flow on a sphere of an electrically conducting and steady viscous incompressible fluid with isothermal surface and uniform heat flux has been considered.

The governing partial differential equations are reduced to locally non-similar partial differential forms by adopting appropriate transformations. The transformed boundary layer equations are solved numerically using implicit finite difference method together with Keller box scheme by Keller (1978) and later by Cebeci and Bradshaw (1984). Here, the attention is focused on the evolution of the surface shear stress in terms of local skin friction and the rate of heat transfer in terms of local Nusselt number, velocity profiles as well as temperature profiles for selected values of parameters consisting of heat radiation parameter Rd, Prandtl number Pr and the surface wall temperature parameter θ_w.

In chapter 2, the effects of radiation on natural convection flow on a sphere have been investigated where the surface of the sphere is isothermal. Here the non-dimensional boundary layer equations are solved by using implicit finite difference methods by Keller (1978), Cebeci and Bradshaw (1984). The results in terms of local skin friction, local Nusselt number will be shown in tabular forms. Velocity profiles, temperature profiles, skin friction coefficient and the rate of heat transfer have been displayed graphically for various values of radiation parameter, surface temperature parameter separately and the Prandtl number as well. Some results for skin friction coefficient and the rate of heat transfer for different values radiation parameter, surface temperature parameter and the Prandtl number have been presented in tabular form. Present numerical results of Nusselt number have been compared with the results of Nazar et al. (2002) and Huang and Chen (1987).

In chapter-3, the effects of radiation on natural convection flow on a sphere with uniform heat flux have been investigated. Numerical results have been shown in terms of local skin friction, rate of heat transfer, velocity profiles as well as temperature profiles for a selection of relevant physical parameters set are shown graphically. Some results for skin friction coefficient and the rate of heat transfer for different values of radiation parameter, surface temperature parameter and the Prandtl number has been presented in tabular form as well.

Chapter 2

Effect of Radiation on Free Convection Flow on a Sphere with Isothermal Surface

2.1 Introduction

In this chapter the effect of radiation on natural convection flow on a sphere with isothermal surface has been investigated. Here a sphere whose surface maintained as isothermal immersed in a viscous incompressible optically thick fluid with radiation heat transfer taken into consideration. The governing boundary layer equations are first transformed into a non-dimensional form and the resulting nonlinear system of partial differential equations are then solved numerically using a very efficient finite-difference method known as the Keller-box scheme. Here we have focused our attention on the evolution of the shear stress in terms of local skin friction and the rate of heat transfer in terms of local Nusselt number, velocity profiles as well as temperature profiles for some selected values of parameter sets consisting of radiation parameter Rd, surface temperature parameter θ_w and the Prandlt number Pr.

2.2 Formulation of the problem

Natural convection boundary layer flow on a sphere of radius *a* of a steady two-dimensional viscous incompressible fluid in presence of radiation heat transfer has been investigated. It is assumed that the surface temperature of the sphere is T_w, where $T_w > T_\infty$. Here T_∞ is the ambient temperature of the fluid, T is the temperature of the fluid in the boundary layer, g is the acceleration due to gravity, r (x) is the radial distance from the symmetrical axis to the surface of the sphere and ($\underline{u}$, $\underline{v}$) are velocity components along the (x, y) axis. The physical configuration considered is as shown in Fig. 2.1:

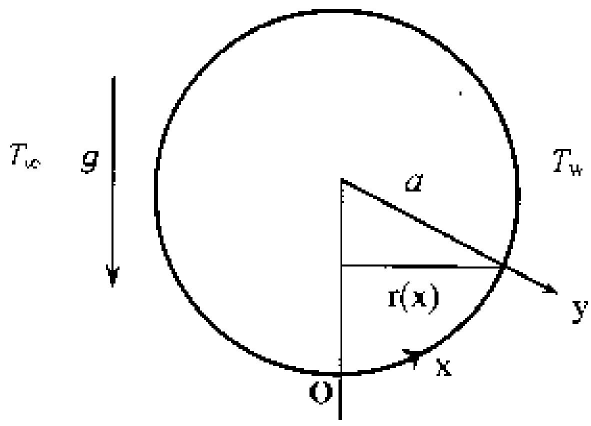

Fig.2.1: Physical model and coordinate system

Under the usual Bousinesq approximation, the equations governing the flow are

$$\frac{\partial}{\partial x}(r\,\underline{u})+\frac{\partial}{\partial y}(r\,\underline{v})=0 \tag{2.1}$$

$$\underline{u}\frac{\partial \underline{u}}{\partial x}+\underline{v}\frac{\partial \underline{u}}{\partial y}=\mu\frac{\partial^2 \underline{u}}{\partial y^2}+\rho g\beta(T-T_\infty)\sin\left(\frac{x}{a}\right) \tag{2.2}$$

$$\underline{u}\frac{\partial T}{\partial x}+\underline{v}\frac{\partial T}{\partial y}=\frac{\kappa}{\rho C_p}\frac{\partial^2 T}{\partial y^2}-\frac{1}{\rho C_p}\frac{\partial q_r}{\partial y} \tag{2.3}$$

The boundary conditions of equation (2.1) to (2.3) are

$$\begin{aligned}&\underline{u}=\underline{v}=0,\ \ T=T_w \quad \text{at} \quad y=0\\ &\underline{u}\to 0,\ \ T\to T_\infty \quad \text{as} \quad y\to\infty\end{aligned} \tag{2.4}$$

where $r(x)=a\,\sin\left(\frac{x}{a}\right)$, g is the acceleration due to gravity. ρ is the density, k is the thermal conductivity, β is the coefficient of thermal expansion, μ is the viscosity of the fluid, C_p is the specific heat due to constant pressure and q_r is the radioactive heat flux in the y direction. In order to reduce the complexity of the problem and to provide a means of comparison with future studies that will employ a more detail representation for the radioactive heat flux, we will consider the optically dense radiation limit. Thus radiative heat flux term is simplified by the Rosseland diffusion approximation, which proposed by Siegel and Howell (1972) and is given by

$$q_r = -\frac{4\sigma}{3(\alpha_r+\sigma_s)}\frac{\partial T^4}{\partial y} \tag{2.5}$$

We now introduce the following non-dimensional variables:

$$\xi = \frac{x}{a}, \quad \eta = Gr^{1/4}\left(\frac{y}{a}\right), \quad u = \frac{a}{\nu}Gr^{-1/2}\underline{u}, \quad v = \frac{a}{\nu}Gr^{-1/4}\underline{v}.$$
$$\theta = \frac{T-T_\infty}{T_w-T_\infty}, \qquad Gr = \frac{g\beta(T_w-T_\infty)a^3}{\nu^2} \tag{2.6}$$

where ν (=μ/ρ) is the reference kinematic viscosity and Gr is the Grashof number, θ is the non-dimensional temperature function .

Substituting variables of (2.6) into equations (2.1)-(2.3) leads to the following non-dimensional equations

$$\frac{\partial}{\partial\xi}(ru)+\frac{\partial}{\partial\eta}(rv)=0 \tag{2.7}$$

$$u\frac{\partial u}{\partial\xi}+v\frac{\partial u}{\partial\eta}=\frac{\partial^2 u}{\partial\eta^2}+\theta\sin\xi \tag{2.8}$$

$$u\frac{\partial\theta}{\partial\xi}+v\frac{\partial\theta}{\partial\eta}=\frac{1}{Pr}\frac{\partial}{\partial\eta}\left[\left\{1+\frac{4}{3}Rd(1+(\theta_w-1)\theta)^3\right\}\frac{\partial\theta}{\partial\eta}\right] \tag{2.9}$$

With the boundary conditions (2.4) become

$$u = v = 0, \quad \theta = 1 \quad \text{at} \quad \eta = 0$$
$$u \to 0, \quad \theta \to 0 \quad \text{as} \quad \eta \to \infty \tag{2.10}$$

where Rd is the radiation-conduction parameter or Plank number, θ_w is the surface heating parameter and Pr is the Prandtl number defined respectively as

$$Rd = \frac{4\sigma T_\infty^3}{k(\alpha_r+\sigma_s)}, \quad \theta_w = \frac{T_w}{T_\infty} \quad \text{and} \quad Pr = \frac{\mu C_p}{k} \tag{2.11}$$

To solve equations (2.7)-(2.9), subject to the boundary conditions (2.10), we assume the following variables

$$\psi = \xi\, r(\xi) f(\xi,\eta), \quad \theta = \theta(\xi,\eta) \tag{2.12}$$

where ψ is the non-dimensional stream function defined in the usual way as

$$u = \frac{1}{r}\frac{\partial\psi}{\partial\eta}, \quad v = -\frac{1}{r}\frac{\partial\psi}{\partial\xi} \tag{2.13}$$

Substituting (2.13) into equations (2.8)-(2.9), after some algebra the transformed equations take the following form

$$\frac{\partial^3 f}{\partial\eta^3} + \left(1 + \frac{\xi}{\sin\xi}\cos\xi\right) f \frac{\partial^2 f}{\partial\eta^2} - \left(\frac{\partial f}{\partial\eta}\right)^2 + \frac{\sin\xi}{\xi}\theta = \xi\left(\frac{\partial f}{\partial\eta}\frac{\partial^2 f}{\partial\xi\partial\eta} - \frac{\partial f}{\partial\xi}\frac{\partial^2 f}{\partial\eta^2}\right) \tag{2.14}$$

$$\frac{1}{Pr}\frac{\partial}{\partial\eta}\left[\left\{1 + \frac{4}{3}Rd\left(1 + \left(\theta_w - 1\right)\theta\right)^3\right\}\frac{\partial\theta}{\partial\eta}\right] + \left(1 + \frac{\xi}{\sin\xi}\cos\xi\right) f \frac{\partial\theta}{\partial\eta} = \xi\left(\frac{\partial f}{\partial\eta}\frac{\partial\theta}{\partial\xi} - \frac{\partial\theta}{\partial\eta}\frac{\partial f}{\partial\xi}\right) \tag{2.15}$$

Along with boundary conditions

$$\begin{aligned} &f = \frac{\partial f}{\partial\eta} = 0, \quad \theta = 1 \quad \text{at} \quad \eta = 0 \\ &\frac{\partial f}{\partial\eta} \to 0, \quad \theta \to 0 \quad \text{as} \quad \eta \to \infty \end{aligned} \tag{2.16}$$

It can be seen that near the lower stagnation point of the sphere i.e. $\xi \approx 0$, equations (2.14) and (2.15) reduce to the following ordinary differential equations:

$$f''' + 2ff'' - f'^2 + \theta = 0 \tag{2.17}$$

$$\frac{1}{Pr}\left[\left\{1 + \frac{4}{3}Rd\left(1 + (\theta_w - 1)\theta\right)^3\right\}\theta'\right]' + 2f\theta' = 0 \tag{2.18}$$

Subject to the boundary conditions

$$\begin{aligned} &f(0) = f'(0) = 0, \quad \theta(0) = 1 \\ &f' \to 0, \quad \theta \to 0 \quad \text{as} \quad y \to \infty \end{aligned} \tag{2.19}$$

In the above equations primes denote differentiation with respect to η.

In practical applications, the physical quantities of principle interest are the shearing stress, the rate of heat transfer and the rate of species concentration transfer in terms of the skin-friction coefficients C_f and Nusselt number Nu respectively, which can be written as

$$C_f = \frac{Gr^{-3/4}a^2}{\mu_\infty v_\infty}(\tau_w)_{y=0} \quad \text{and} \quad Nu = \frac{aGr^{-1/4}}{k(T_w - T_\infty)}(q_c + q_r)_{y=0} \tag{2.20}$$

$$\text{where} \quad \tau_w = \mu\left(\frac{\partial u}{\partial y}\right) \quad \text{and} \quad q_c = -k\left(\frac{\partial T}{\partial y}\right) \text{ is the conduction heat flux.} \tag{2.21}$$

Using the variables (2.6) and (2.13) and the boundary condition (2.19) into (2.20)-(2.21), we get

$$C_f = \xi f''(\xi,0) \tag{2.22}$$

$$Nu = -\left(1 + \frac{4}{3}Rd\theta_w^3\right)\theta'(\xi,0) \tag{2.23}$$

The values of the velocity and temperature distribution are calculated respectively from the following relations:

$$u = \frac{\partial f}{\partial \eta}, \quad \theta = \theta(\xi,\eta) \tag{2.24}$$

2.3 Method of Solution

To get the solutions of the parabolic differential equations (2.14) and (2.15) along with the boundary condition (2.16), we shall employ a most practical, an efficient and accurate solution technique, known as implicit finite difference method together with Keller- box scheme which is well documented and widely used by Keller and Cebeci (1971) and recently by Hossain (1992) and Hossain et al. (1998).

To employ the finite difference method, the system of partial differential equations considered here are first converted to a system of five first order partial differential equations by introducing new unknown functions of η derivatives.

Here we first convert the equations (2.14), (2.15) and their boundary condition into the system of first order equations. For this purpose we introduce new dependent variables

$u(\xi, \eta)$, $v(\xi, \eta)$ and $p(\xi, \eta)$ so that the transformed momentum and energy equations can be written as

$$f' = u \tag{2.25}$$

$$u' = v \tag{2.26}$$

$$g' = p \tag{2.27}$$

$$v' + p_1 fv - p_2 u^2 + p_3 g = \xi\left(u\frac{\partial u}{\partial \xi} - \frac{\partial f}{\partial \xi}v\right) \tag{2.28}$$

$$\frac{1}{\Pr}\left(1+\frac{4}{3}p_4\right)p' + \frac{4}{pr}p_4 g^2 p^2 + p_1 fp = \xi\left(u\frac{\partial g}{\partial \xi} - p\frac{\partial f}{\partial \xi}\right) \tag{2.29}$$

$$p_1 = 1+\frac{\xi}{\sin\xi}\cos\xi \ ;\ p_2 = 1,\ \ p_3 = \frac{\sin\xi}{\xi}\ ,\ p_4 = Rd\left\{1+(\theta_w - 1)\right\}^3 \tag{2.30}$$

and the boundary conditions are

$$\begin{aligned} &f(\xi, 0) = 0,\ u(\xi, 0) = 0 \text{ and } g(\xi, 0) = 1 \\ &u(\xi, \infty) = 0,\ g(\xi, \infty) = 0 \end{aligned} \tag{2.31}$$

We now consider the net rectangle on the (ξ, η) plane shown in the figure A1 (Appendix) and denote the net points by

$$\begin{aligned} &\xi^0 = 0, \quad \xi^n = \xi^{n-1} + k_n, \ n = 1,2,\ldots N \\ &\eta_0 = 0, \ \eta_j = \eta_{j-1} + h_j, \quad j = 1,2,\ldots J \end{aligned} \tag{2.32}$$

Here 'n' and 'j' are just sequence of numbers on the (ξ, η) plane, k_n and h_j are the variable mesh widths.

We approximate the quantities f, u, v, p at the points (ξ^n, η_j) of the net by f^n_j, u^n_j, v^n_j, p^n_j which we call net functions. We also employ the notation g^n_j for the quantities midway between net points shown in figure A1 (appendix) and for any net function as

$$\xi^{n-1/2} = \frac{1}{2}(\xi^n + \xi^{n-1}) \tag{2.33}$$

$$\eta_{j-1/2} = \frac{1}{2}(\eta_j + \eta_{j-1}) \tag{2.34}$$

$$g_j^{n-1/2} = \frac{1}{2}(g_j^n + g_j^{n-1}) \tag{2.35}$$

$$g_{j-1/2}^n = \frac{1}{2}(g_j^n + g_{j-1}^n) \tag{2.36}$$

The finite difference approximations according to Box method to the three first order ordinary differential equations (2.25)-(2.27) are written for the mid point (ξ^n, $\eta_{j-1/2}$) of the segment P_1P_2 shown in the figureA1 (appendix) and the finite difference approximations to the two first order differential equations (2.28)-(2.29) are written for the mid point

($\xi^{n-1/2}$, $\eta_{j-1/2}$) of the rectangle $P_1P_2P_3P_4$. Central difference approximations made such that those equations involving ξ explicitly are centered at ($\xi_{i-1/2}$, $\eta_{j-1/2}$) and the remainders at

(ξ_i, $\eta_{j-1/2}$), where $\eta_{j-1/2} = (\eta_j + \eta_{j-1})$ etc. This leads to a set of non-linear difference equations for the unknowns in terms of their values at ξ_{i-1}. This procedure yields.

$$\begin{aligned}
&\frac{1}{2}\left(\frac{v_j^n - v_{j-1}^n}{h_j} + \frac{v_j^{n-1} - v_{j-1}^{n-1}}{h_j}\right) + (p_1 fv)_{j-1/2}^{n-1/2} - (p_2 u^2)_{j-1/2}^{n-1/2} \\
&+(p_3 g)_{j-1/2}^{n-1/2} = \xi_{j-1/2}^{n-1/2}\Big(u_{j-1/2}^{n-1/2} \frac{u_{j-1/2}^n - u_{j-1/2}^{n-1}}{k_n} \\
&-v_{j-1/2}^{n-1/2} \frac{f_{j-1/2}^n - f_{j-1/2}^{n-1}}{k_n}\Big)
\end{aligned} \tag{2.37}$$

$$\frac{1}{2P_r}\left(1+\frac{4}{3}p_4\right)\left(\frac{p_j^n-p_{j-1}^n}{h_j}+\frac{p_j^{n-1}-p_{j-1}^{n-1}}{h_j}\right)+(p_1 fp)_{j-1/2}^{n-1/2}$$
$$+\frac{4}{P_r}(p_4(gp)^2)_{j-1/2}^{n-1/2}=\xi_{j-1/2}^{n-1/2}\ (u_{j-1/2}^{n-1/2}\frac{g_{j-1/2}^n-g_{j-1/2}^{n-1}}{k_n} \tag{2.38}$$
$$-p_{j-1/2}^{n-1/2}\frac{f_{j-1/2}^n-f_{j-1/2}^{n-1}}{k_n}\ )$$

Now from the equation (2.37) we get

$$\Rightarrow h_j^{-1}(v_j^n-v_{j-1}^n)+\left\{(p_1)_{j-1/2}^n+\alpha_n\right\}(fv)_{j-1/2}^n-\left\{(p_2)_{j-1/2}^n+\alpha_n\right\}$$
$$(u^2)_{j-1/2}^n+(p_3)_{j-1/2}^n(g)_{j-1/2}^n+\alpha_n(v_{j-1/2}^{n-1}f_{j-1/2}^n \tag{2.39}$$
$$-v_{j-1/2}^n f_{j-1/2}^{n-1})=R_{j-1/2}^{n-1}$$

Again from the equation (2.38) we get

$$\Rightarrow\frac{1}{P_r}\left(1+\frac{4}{3}p_4\right)h_j^{-1}(p_j^n-p_{j-1}^n)+\left\{(p_1)_{j-1/2}^{n-1/2}+\alpha_n\right\}(fp)_{j-1/2}^n$$
$$+\frac{4}{P_r}\left\{(p_4)_{j-1/2}^n((gp)^2)_{j-1/2}^n\right\}+\alpha_n(u_{j-1/2}^n g_{j-1/2}^{n-1} \tag{2.40}$$
$$-u_{j-1/2}^{n-1}g_{j-1/2}^n-p_{j-1/2}^n f_{j-1/2}^{n-1}+p_{j-1/2}^{n-1}f_{j-1/2}^n)=T_{j-1/2}^{n-1}$$

The boundary conditions become

$$f_0^n=0 \qquad u_0^n=0 \quad p_0^n=1$$
$$u_J^n=0 \qquad g_J^n=0 \tag{2.41}$$

If we assume $f_j^{n-1}, u_j^{n-1}, v_j^{n-1}, g_j^{n-1}, p_j^{n-1}$ to be known for $0\le j\le J$, equations (2.25) to (2.27) and (2.28) – (2.29) form a system of $5J+5$ non linear equations for the solutions of the $5J+5$ unknowns ($f_j^n, u_j^n, v_j^n, g_j^n, p_j^n$), j = 0,1,2 …J.

These non-linear systems of algebraic equations are to be linearized by Newton's Quassy linearization method (ref. appendix).

2.4 Results and discussion

Here we have been investigated the effect of radiation on natural convection flow on a sphere with isothermal surface for different values of relevant physical parameters. Solutions are obtained for fluids having Prandtl number Pr = 0.72 (air) and for some test values of Pr = 1.0. 1.74, 2.0, 3.0 against η for a wide range of values of radiation parameter Rd. The values of radiation parameter Rd =1.0, 2.0, 3.0, 4.0 and 5.0 have been taken while Pr = 1.0 and θ_w = 1.1. Different values of surface temperature parameter θ_w = 1.1, 1.2, 1.3, 1.4 and 1.5 are considered while Pr = 0.72 and Rd =1.0. Numerical values of local rate of heat transfer are calculated in terms of Nusselt number Nu for the surface of the sphere from lower stagnation point to upper stagnation point. The effect for different values of radiation parameter Rd on local skin friction coefficient C_f and the local Nusselt number Nu, as well as velocity and temperature profiles with the Prandtl number Pr = 1.0 and surface temperature parameter

θ_w = 1.1

Figures 2.2-2.3 display results for the velocity and temperature profiles, for different values of radiation parameter Rd while Prandtl number Pr = 0.72 and surface temperature parameter θ_w = 1.1. It has been seen from figures 2.2 and 2.3 that as the radiation parameter Rd increase, the velocity and the temperature increase. The changes of velocity profiles in the η direction reveals the typical velocity profile for natural convection boundary layer flow i,e the velocity is zero at the boundary wall then the velocity increases to the peak value as η increases and finally the velocity approaches to zero (the asymptotic value).The maximum values of velocity are recorded to be 0.41262, 0.46612, 0.50142, 0.52804 and 0.54940 for Rd=1.0, 2.0, 3.0, 4.0 and 5.0 respectively which occur in between the points η = 1.23788 and η=1.30254. Here, it is observed that at η = 1.23788, the velocity increases by 33.149%. The changes of temperature profiles in the η direction also shows the typical temperature profile for natural convection boundary layer flow that is the value of temperature is 1.0 (one) at the boundary wall then the temperature decreases gradually along η direction to the asymptotic value.

The effect for different values of surface temperature parameter θ_w, the velocity and temperature profiles while Prandtl number Pr = 0.72 and radiation-conduction parameter Rd =1.0 are shown in the figures 2.4 and 2.5. Here, surface temperature parameter θ_w increases, the velocity and the temperature increases slightly such that there exists a local minimum of the velocity within the boundary layer, but velocity increases near the surface of the sphere and then temperature decreases slowly and finally approaches to zero. However, in the figures 2.6 and 2.7, we are shown that when the Prandtl number Pr = 0.72, 1,0, 1.74, 2.0 and 3.0 increases with θ_w = 1.1 and Rd =1.0 both the velocity and temperature decrease.

Figures 2.8-2.9 show that skin friction coefficient C_f and heat transfer coefficient Nu increases for increasing values of radiation parameter Rd. while Prandtl number Pr = 0.72 and surface temperature parameter θ_w = 1.1. The values of skin friction C_f and Nusselt number Nu are recorded to be 1.01293, 1.07813, 1.11961, 1.4994, 1.17325 and 0.77080. 1.03282, 1.25211, 1.44365. 1.61637 for Rd=1.0, 2.0, 3.0, 4.0 and5.0 respectively which occur at the same point ξ = 1.57080. Here, it is observed that at ξ = 1.57080, the skin friction increases by 15.827% and Nusselt number Nu increases by 109.7%. It is observed from the figure 2.8 that the skin friction increases gradually from zero value at lower stagnation point along the ξ direction and from figure 2.9, it reveals that the rate of heat transfer increases slightly along the ξ direction from lower stagnation point to the downstream.

From figures 2.10 - 2.11, it can also easily be seen that an increase in the surface temperature parameter θ_w leads to increase the local skin friction coefficient C_f and the local rate of heat transfer Nu slightly while Prandtl number Pr = 0.72 and radiation parameter Rd =1.0.Also it is observed that at any position of ξ, the skin friction coefficient C_f and the local Nusselt number Nu increase as θ_w increases from 1.1 to 1.5. This phenomenon can easily be understood from the fact that when the surface temperature parameter θ_w increases, the temperature of the fluid rises and the thickness of the velocity boundary layer grows i.e. the thermal boundary layer becomes thinner than the velocity boundary layer. Therefore the skin friction coefficient C_f and the local Nusselt number Nu increase.

The variation of the local skin friction coefficient C_f and local rate of heat transfer Nu for different values of Prandtl number Pr while θ_w = 1.1 and Rd =1.0 are shown in the figures 2.12 and 2.13. We can observe from the figures that as the Prandtl number Pr increases, the skin friction coefficient decreases and heat transfer coefficient increases but the rate of increase in the heat transfer coefficient is higher than that of the skin friction coefficient so, the effect of Prandtl number Pr on heat transfer coefficient is more than that of the effect of Pr on skin friction coefficient.

Numerical values of skin friction coefficient C_f and rate of heat transfer Nu are calculated from equations (2.22) and (2.23) for the surface of the sphere from lower stagnation point to upper stagnation point. Numerical values of C_f and Nu are depicted in Table 2.1, 2.2 and 2.3

Table 2. 1: Skin friction coefficient and rate of heat transfer against ξ for different values of Prandtl numbers and against fixed radiation parameters Rd = 1.0 and θ_w=1.1.

	Pr = 0.72		Pr = 1.00		Pr = 1.74		Pr = 3.00	
ξ	C_f	Nu	C_f	Nu	C_f	Nu	C_f	Nu
0.00000	0.00000	0.84401	0.00000	0.95813	0.00000	1.17629	0.00000	1.42297
0.10472	0.09245	0.84325	0.08839	0.95727	0.08131	1.17524	0.07431	1.42172
0.20944	0.18427	0.84110	0.17619	0.95484	0.16208	1.17227	0.14813	1.41815
0.31416	0.27485	0.83756	0.26280	0.95082	0.24177	1.16738	0.22098	1.41227
0.40143	0.34895	0.83353	0.33366	0.94626	0.30699	1.16182	0.28060	1.40559
0.50615	0.43568	0.82739	0.41663	0.93932	0.38336	1.15335	0.35044	1.39542
0.61087	0.51949	0.81983	0.49681	0.93076	0.45719	1.14292	0.41798	1.38289
0.71558	0.59979	0.81082	0.57366	0.92055	0.52800	1.13048	0.48277	1.36795
0.80285	0.66362	0.80219	0.63478	0.91078	0.58434	1.11857	0.53435	1.35365
0.90757	0.73604	0.79045	0.70415	0.89749	0.64834	1.10238	0.59299	1.33422
1.01229	0.80341	0.77718	0.76874	0.88248	0.70799	1.08409	0.64769	1.31227
1.20428	0.91212	0.74873	0.87309	0.85028	0.80457	1.04489	0.73642	1.26525
1.30900	0.96246	0.73088	0.92151	0.83008	0.84954	1.02030	0.77785	1.23576
1.46608	1.02485	0.70082	0.98171	0.79607	0.90570	0.97893	0.82981	1.18619
1.57080	1.05705	0.67848	1.01293	0.77080	0.93506	0.94820	0.85717	1.14938

Table 2.2: Skin friction coefficient and rate of heat transfer against ξ for different values of radiation parameter against fixed Prandtl number Pr = 1.0 and θ_w=1.1.

	Rd = 1.00		Rd = 2.00		Rd = 3.00		Rd=5.00	
ξ	C_f	Nu	C_f	Nu	C_f	Nu	C_f	Nu
0.00000	0.00000	0.95813	0.00000	1.28514	0.00000	1.55857	0.00000	2.01387
0.10472	0.08839	0.95727	0.09440	1.28398	0.09824	1.55717	0.10323	2.01205
0.20944	0.17619	0.95484	0.18815	1.28071	0.19580	1.55319	0.20574	2.00689
0.31416	0.26280	0.95082	0.28062	1.27530	0.29203	1.54663	0.30684	1.99838
0.40143	0.33366	0.94626	0.35627	1.26916	0.37074	1.53917	0.38952	1.98871
0.50615	0.41663	0.93932	0.44481	1.25981	0.46284	1.52782	0.48625	1.97400
0.61087	0.49681	0.93076	0.53035	1.24828	0.55180	1.51382	0.57965	1.95585
0.71558	0.57366	0.92055	0.61230	1.23455	0.63700	1.49714	0.66907	1.93422
0.80285	0.63478	0.91078	0.67742	1.22138	0.70469	1.48116	0.74007	1.91350
0.90757	0.70415	0.89749	0.75130	1.20349	0.78144	1.45943	0.82052	1.88533
1.01229	0.76874	0.88248	0.82001	1.18327	0.85276	1.43487	0.89523	1.85347
1.20428	0.87309	0.85028	0.93079	1.13991	0.96761	1.38221	1.01533	1.78517
1.30900	0.92151	0.83008	0.98205	1.11269	1.02064	1.34914	1.07063	1.74228
1.46608	0.98171	0.79607	1.04548	1.06687	1.08608	1.29348	1.14502	1.66143
1.57080	1.01293	0.77080	1.07813	1.03282	1.11961	1.25211	1.17325	1.61637

Table 2. 3: Skin friction coefficient and rate of heat transfer against ξ for different values of wall temperature θ_w against fixed radiation number Rd = 1.0 and Prandtl number Pr=0.72.

	θ_w=1.1		θ_w = 1.2		θ_w = 1.4		θ_w = 1.5	
ξ	C_f	Nu	C_f	Nu	C_f	Nu	C_f	Nu
0.00000	0.00000	0.84401	0.00000	0.90655	0.00000	1.04700	0.00000	1.12426
0.10472	0.09245	0.84325	0.09426	0.90574	0.09775	1.04605	0.09941	1.12325
0.20944	0.18427	0.84110	0.18787	0.90342	0.19483	1.04338	0.19814	1.12037
0.31416	0.27485	0.83756	0.28021	0.89961	0.29059	1.03897	0.29552	1.11563
0.40143	0.34895	0.83353	0.35575	0.89528	0.36892	1.03395	0.37516	1.11025
0.50615	0.43568	0.82739	0.44417	0.88868	0.46059	1.02632	0.46838	1.10205
0.61087	0.51949	0.81983	0.52960	0.88055	0.54914	1.01691	0.55842	1.09195
0.71558	0.59979	0.81082	0.61144	0.87085	0.63396	1.00570	0.64465	1.07990
0.80285	0.66362	0.80219	0.67649	0.86156	0.70137	0.99495	0.71317	1.06835
0.90757	0.73604	0.79045	0.75029	0.84894	0.77781	0.98034	0.79086	1.05266
1.01229	0.80341	0.77718	0.81892	0.83467	0.84887	0.96382	0.86307	1.03491
1.20428	0.91212	0.74873	0.92962	0.80407	0.96339	0.92841	0.97938	1.99686
1.30900	0.96246	0.73088	0.98085	0.78486	1.01631	0.90617	1.03310	1.97296
1.46608	1.02485	0.70082	1.04429	0.75252	1.08172	0.86873	1.09941	1.93273
1.57080	1.05705	0.67848	1.07696	0.72848	1.11529	0.84090	1.13340	1.90281

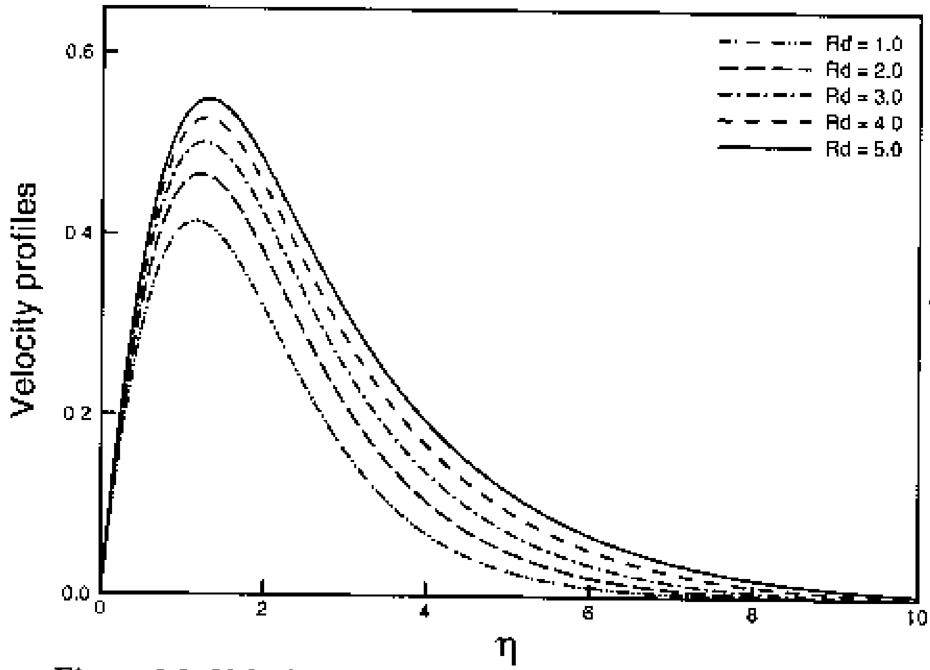

Figure 2.2: Velocity profiles for different values of Rd while θ_w =1.1 and Pr=0.72.

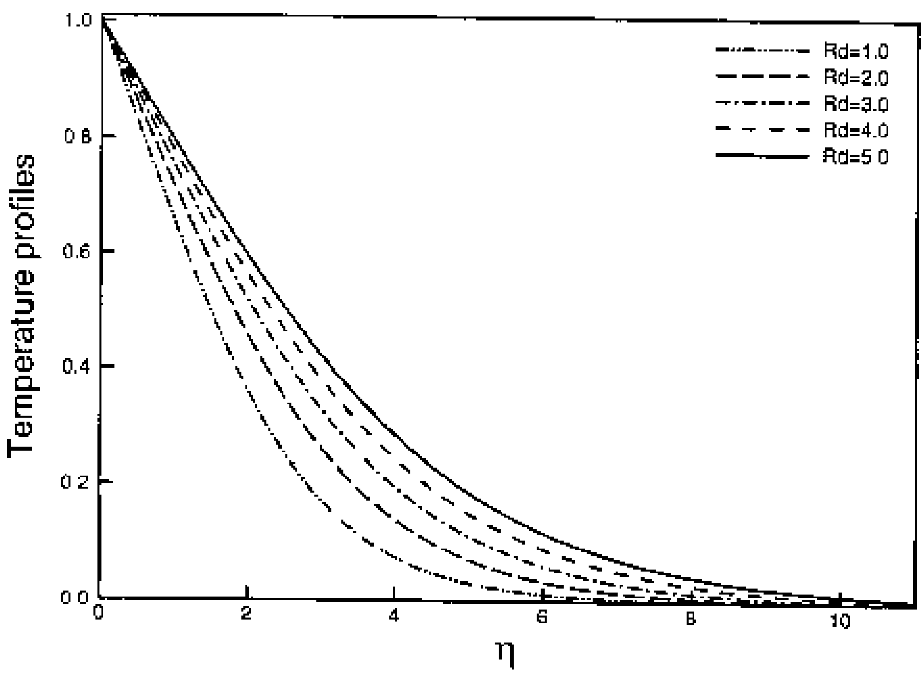

Figure 2.3: Temperature profiles for different values of Rd while θ_w =1.1 and Pr=0.72.

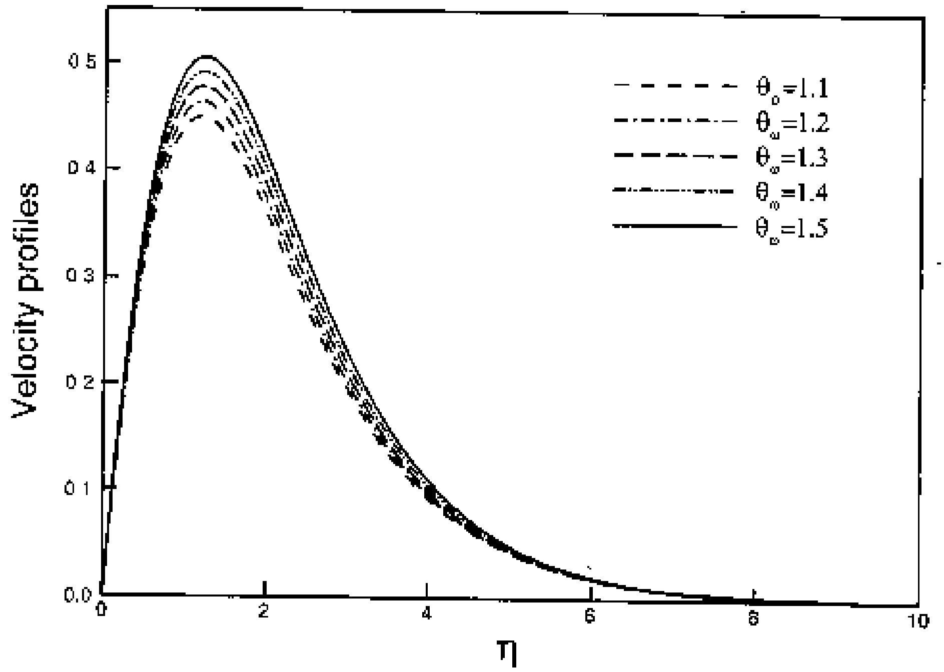

Figure 2.4: Velocity profiles for different values of θ_w while Rd =1.0 and Pr=0.72.

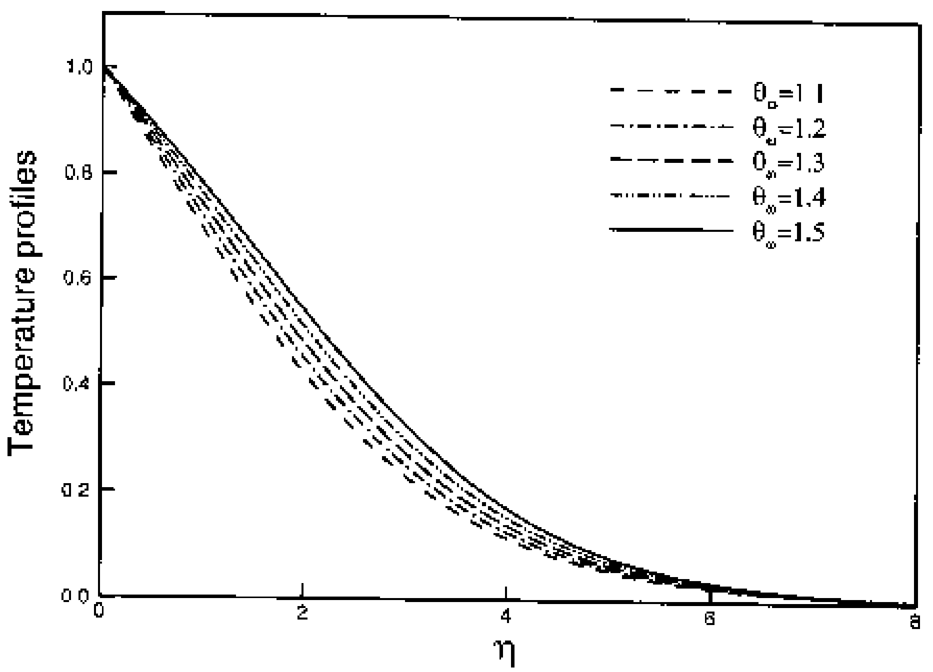

Figure 2.5: Temperature profiles for different values of θ_w while Rd =1.0 and Pr=0.72.

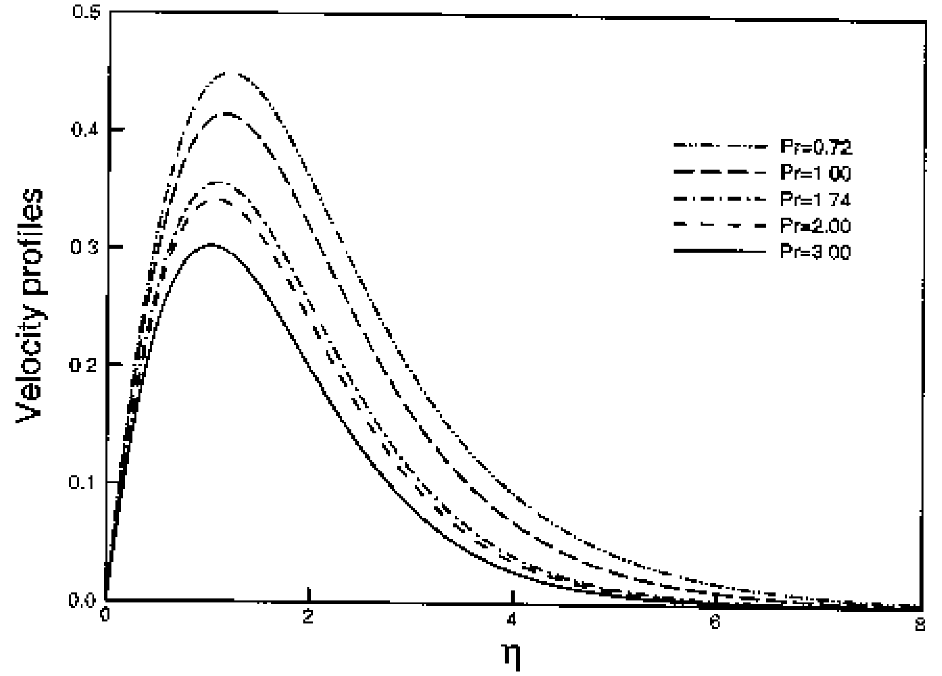

Figure 2.6: Velocity profiles for different values of Pr while θ_w=1.1 and Rd = 1.0.

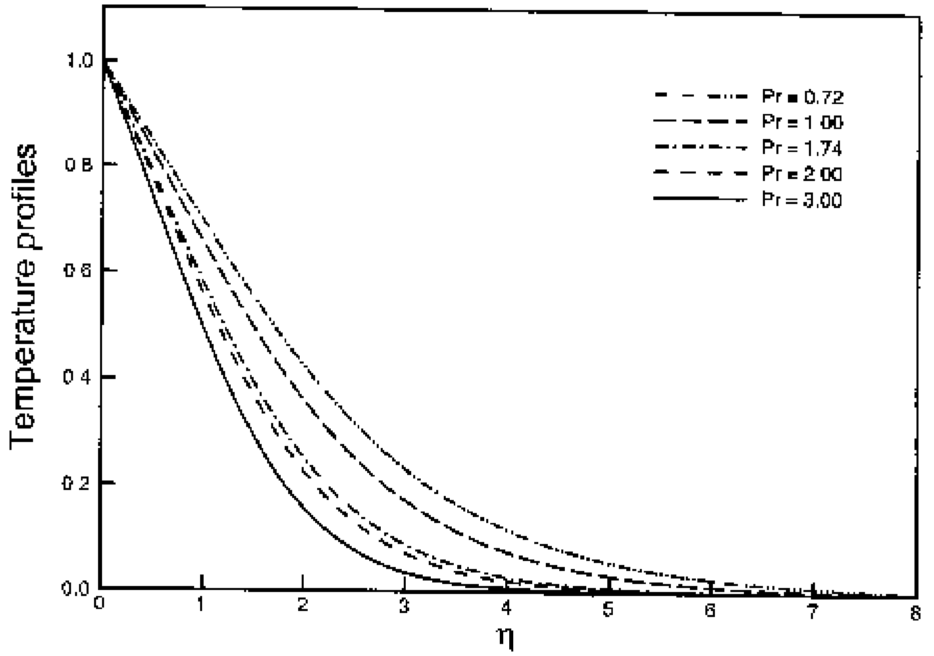

Figure 2.7: Temperature profiles for different values of Pr while θ_w =1.1 and Rd=1.0.

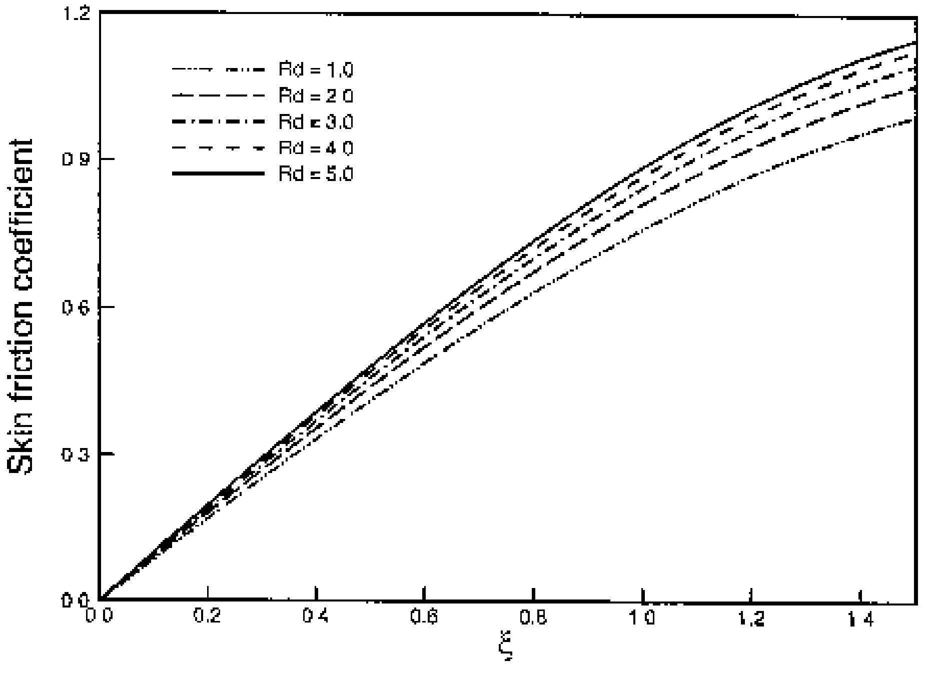

Figure 2.8: Skin friction coefficients for different values Rd while $\theta_w = 1.1$ and Pr =0.72

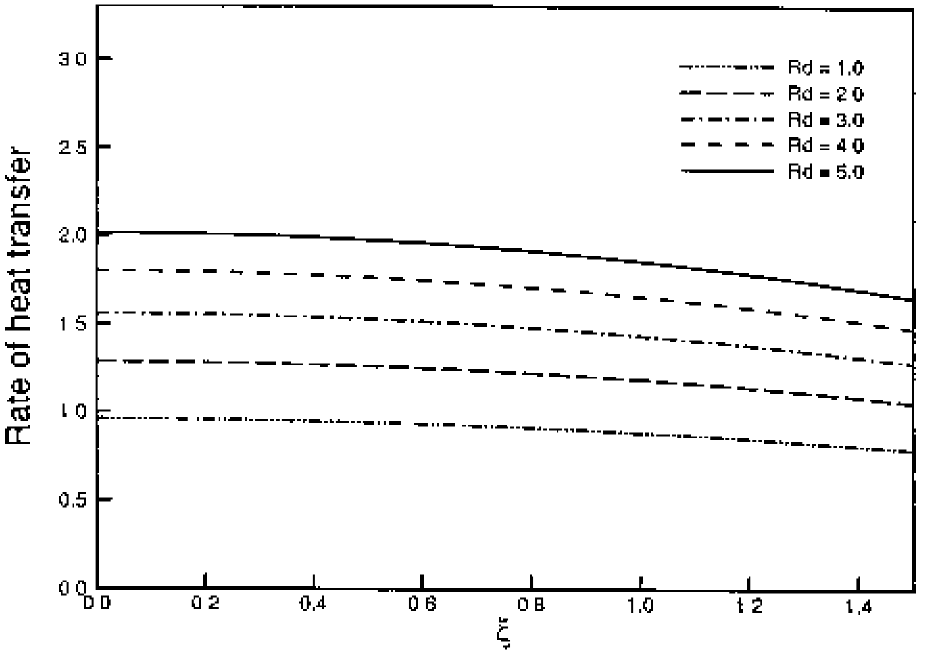

Figure 2.9: Rate of heat transfer for different values of Rd while $\theta_w = 1.1$ and Pr =0.72

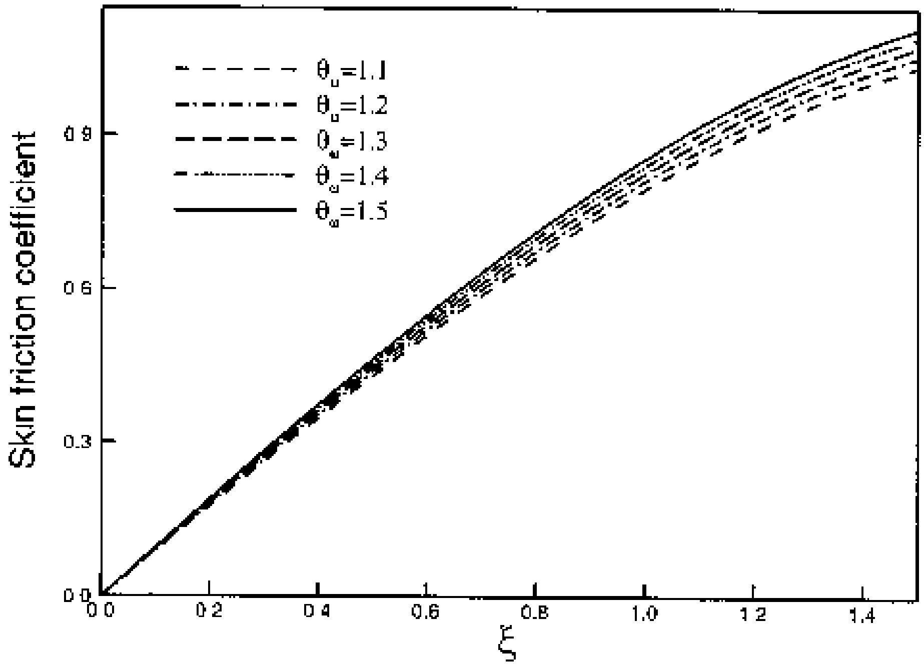

Figure 2.10: Skin friction coefficients for different values of θ_w while Rd= 1.1 and Pr =0.72

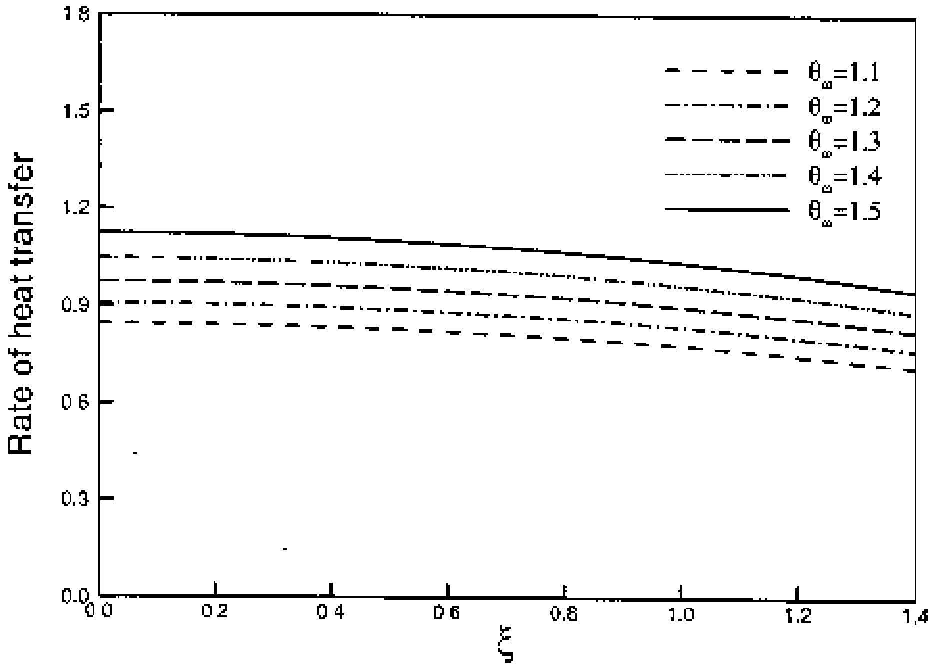

Figure 2.11: Rate of heat transfer for different values of θ_w while Rd= 1.1 and Pr =0.72

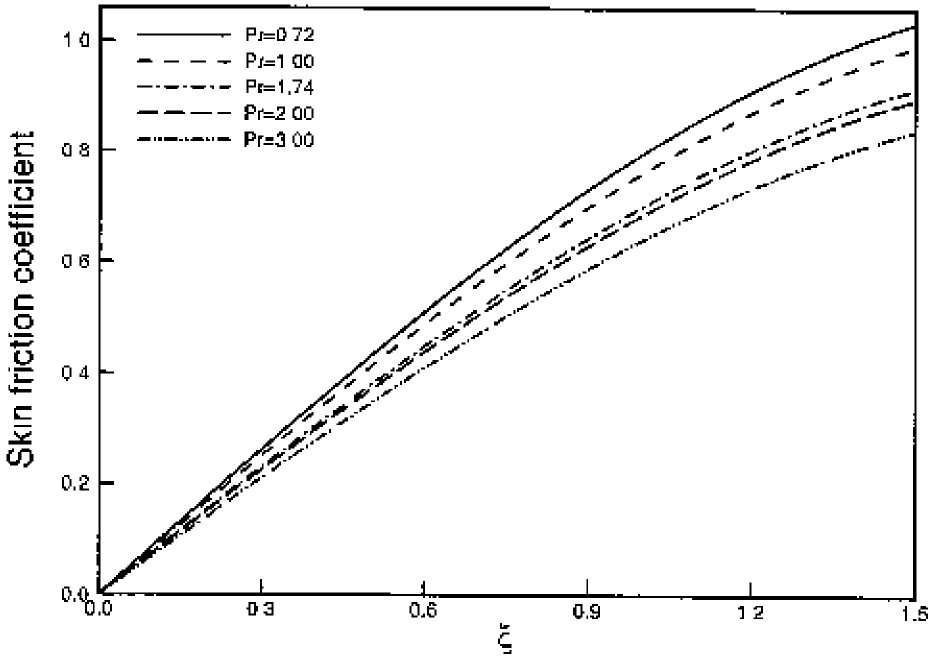

Figure 2.12: Skin friction coefficients for different values of Pr while Rd=1.0 and θ_w = 1.1.

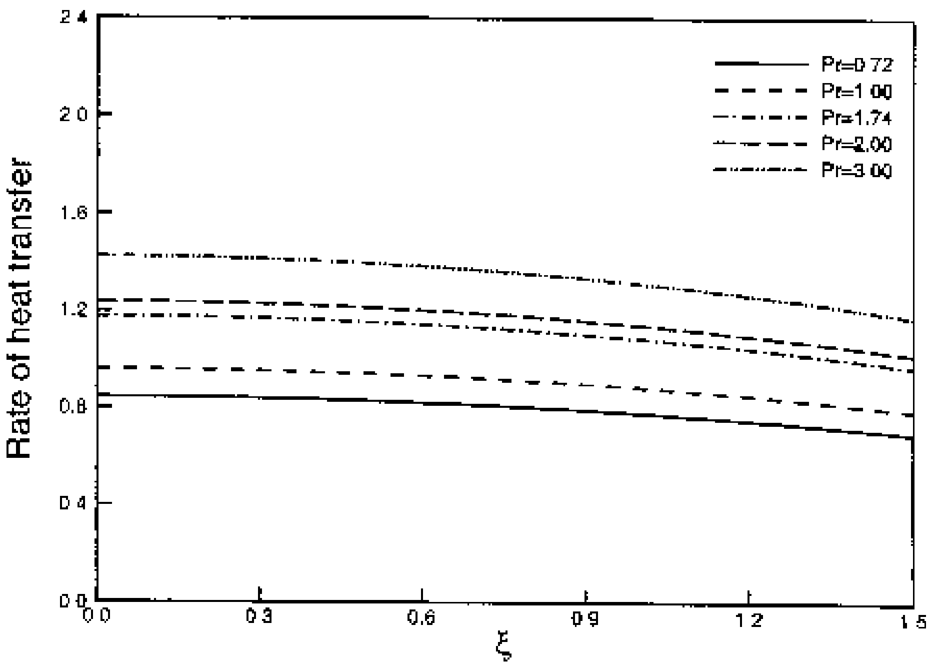

Figure 2.13: Rate of heat transfer for different values of Pr while Rd=1.0 and θ_w = 1.1.

2.5 Comparison of the results

Figure 2.14 depicts the comparisons of the present numerical results of the Nusselt number Nu with those obtained by Nazar et al. (2002) and Huang and Chen (1987). Here, the radiation effect has been ignored (i.e., Rd =0.0) and Prandtl numbers Pr = 0.7 and 7.0 are chosen. I studied well the results and it helped me to take firm decision that the present results agreed well with the solutions of Nazar et al. (2002) and Huang and Chen (1987) in the absence of suction and blowing.

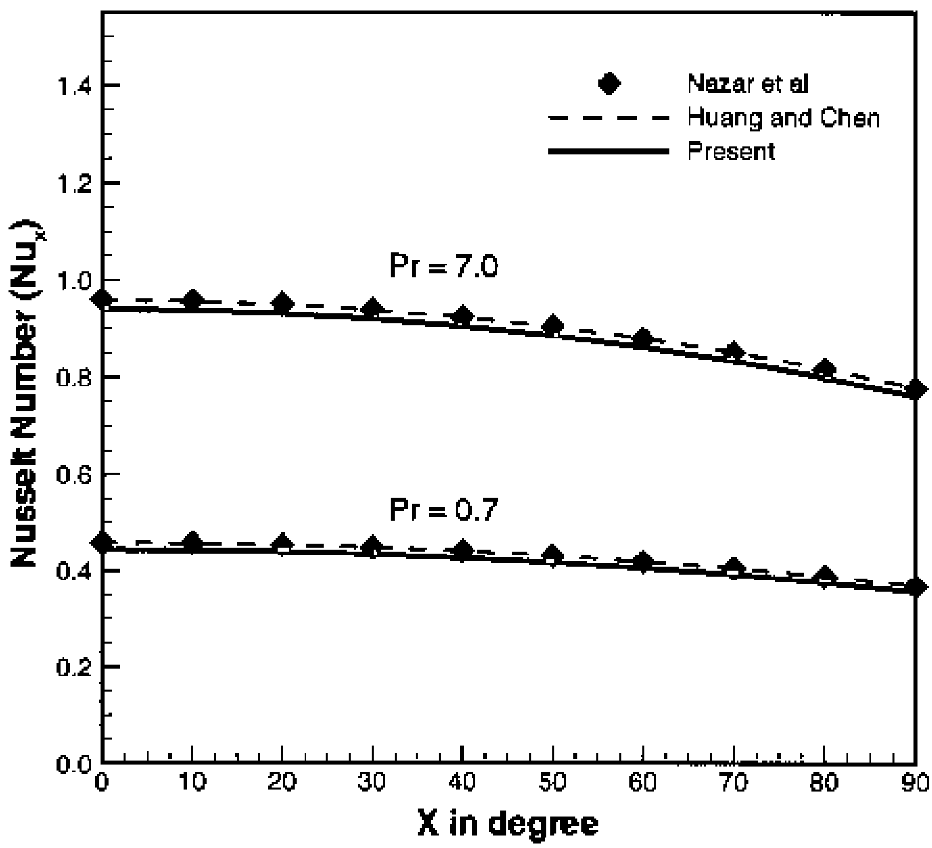

Figure 2.14: Comparisons of the present numerical results of Nusselt number Nu for the Prandtl numbers Pr = 0.7, 7.0 with those obtained by Nazar et al. (2002) and Huang and Chen (1987).

2.6 Conclusion

The effect of radiation on natural convection flow on a sphere with isothermal surface has been investigated for different values of relevant physical parameters including Prandtl number Pr, and surface temperature parameter θ_w.

Here we have transformed the governing boundary layer equations of motion into a non-dimensional form and the resulting non-linear systems of partial differential equations are reduced to local non-similarity boundary layer equations, which are solved numerically by using implicit finite difference method together with the Keller-box scheme. From the present investigation we can draw the following conclusions:

- Significant effects of radiation parameter Rd on velocity and temperature profiles as well as on skin friction and the rate of heat transfer have been found in this investigation. An increase in the values of radiation parameter Rd leads to both the velocity and the temperature profiles increase, the local skin friction coefficient C_f and the local rate of heat transfer Nu also increases for increase of Rd at different position of ξ for Pr=1.0 and θ_w=1.1.
- All the velocity profile, temperature profile, the local skin friction coefficient C_f and the local rate of heat transfer Nu increase significantly when the values of surface temperature parameter θ_w increases while Rd=1.0 and Pr=0.72
- For increasing values of Prandtl number Pr leads to decrease the velocity profile and the local skin friction coefficient C_f, but the temperature profile and the local rate of heat transfer Nu increases as the increase of the Prandtl number while Rd=1.0 and Pr=0.72.

Chapter 3

Effect of Radiation on Free Convection Flow on a Sphere with Uniform Surface Heat flux

3.1 Introduction

The effect of radiation on natural convection flow on a sphere with uniform surface heat flux has been investigated in this chapter. We have considered here a sphere immersed in a viscous incompressible optically thick fluid with uniform heat flux. Here the governing boundary layer equations are first transformed into a non-dimensional form and the resulting nonlinear system of partial differential equations are then solved numerically using a very efficient finite-difference method known as the Keller-box scheme. Here we have focused our attention on the evolution of the shear stress in terms of local skin friction and the rate of heat transfer in terms of local Nusselt number, velocity profiles as well as temperature profiles for some selected values of parameter sets consisting of radiation parameter Rd, surface temperature parameter θ_w and the Prandlt number Pr.

3.2 Formulation of the problem

Natural convection boundary layer flow on a sphere of radius a of a steady two-dimensional viscous incompressible fluid in presence of radiation heat transfer has been investigated. It is assumed that the surface temperature of the sphere is T_w, where $T_w > T_\infty$. Here T_∞ is the ambient temperature of the fluid. T is the temperature of the fluid in the boundary layer, g is the acceleration due to gravity, r (x) is the radial distance from the symmetrical axis to the surface of the sphere and ($\underline{u}$, $\underline{v}$) are velocity components along the (x, y) axis. The physical configuration considered is as shown in Fig. 3.1:

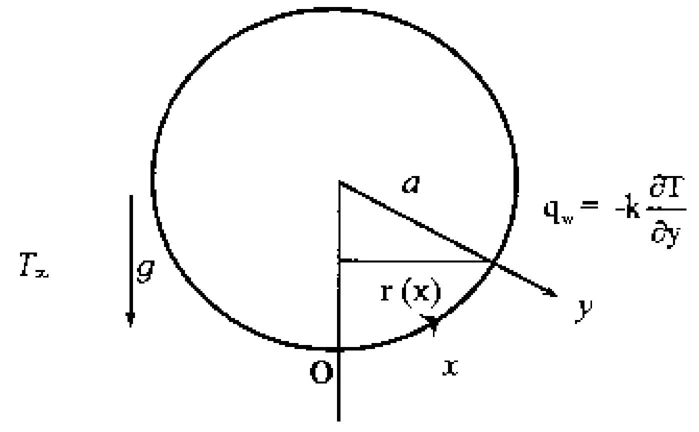

Fig. 3.1: Physical model and coordinate system

Under the usual Bousinesq approximation, the equations those govern the flow are

$$\frac{\partial}{\partial x}(r\underline{u})+\frac{\partial}{\partial y}(r\underline{v})=0 \tag{3.1}$$

$$\underline{u}\frac{\partial \underline{u}}{\partial x}+\underline{v}\frac{\partial \underline{u}}{\partial y}=\mu\frac{\partial^2 \underline{u}}{\partial y^2}+\rho g\beta(T-T_\infty)\sin\left(\frac{x}{a}\right) \tag{3.2}$$

$$\underline{u}\frac{\partial T}{\partial x}+\underline{v}\frac{\partial T}{\partial y}=\frac{k}{\rho C_p}\frac{\partial^2 T}{\partial y^2}-\frac{1}{\rho C_p}\frac{\partial q_r}{\partial y} \tag{3.3}$$

The boundary conditions of equation (3.1) to (3.3) are

$$\begin{aligned} &\underline{u}=\underline{v}=0,\ \ q_w=-k\frac{\partial T}{\partial y}\ \ \text{at}\ \ y=0 \\ &\underline{u}\to 0,\ \ T\to T_\infty\ \ \text{as}\ \ \ y\to\infty \end{aligned} \tag{3.4}$$

where g is the acceleration due to gravity, ρ is the density, k is the thermal conductivity.β is the coefficient of thermal expansion, μ is the viscosity of the fluid, C_p is the specific heat due to constant pressure and q_r is the radiative heat flux in the y direction. In order to reduce the complexity of the problem and to provide a means of comparison with future studies that will employ a more detail representation for the radiative heat flux, we will consider the optically dense radiation limit. Thus the Rosseland diffusion approximation proposed by Siegel and Howell (1972) and is given by simplifies radiation heat flux term as:

$$q_r = -\frac{4\sigma}{3(\alpha_r + \sigma_s)}\frac{\partial T^4}{\partial y} \tag{3.5}$$

We now introduce the following non-dimensional variables:

$$\xi = \frac{x}{a}, \quad \eta = Gr^{1/5}\left(\frac{y}{a}\right), \quad u = \frac{a}{\nu}Gr^{-2/5}\underline{u}, \quad v = \frac{a}{\nu}Gr^{-1/5}\underline{v},$$
$$\theta = Gr^{1/5}\frac{T-T_\infty}{aq_w/k}, \qquad Gr = g\beta\left(aq_w/k\right)\frac{a^4}{\nu^2} \tag{3.6}$$

where ν (=μ/ρ) is the reference kinematic viscosity and Gr is the Grashof number, θ is the non-dimensional temperature function .

Substituting variable (3.6) into equations (3.1)-(3.3) leads to the following non-dimensional equations

$$\frac{\partial}{\partial\xi}(ru) + \frac{\partial}{\partial\eta}(rv) = 0 \tag{3.7}$$

$$u\frac{\partial u}{\partial\xi} + v\frac{\partial u}{\partial\eta} = \frac{\partial^2 u}{\partial\eta^2} + \theta\sin\xi \tag{3.8}$$

$$u\frac{\partial\theta}{\partial\xi} + v\frac{\partial\theta}{\partial\eta} = \frac{1}{Pr}\frac{\partial}{\partial\eta}\left[\left\{1 + \frac{4}{3}Rd(1+\Delta\theta)\right\}\frac{\partial\theta}{\partial\eta}\right] \tag{3.9}$$

With the boundary conditions (3.4) as

$$u = v = 0, \quad \frac{\partial\theta}{\partial\eta} = -1 \quad \text{at} \quad \eta = 0$$
$$u \to 0, \quad \theta \to 0 \quad \text{as} \quad \eta \to \infty \tag{3.10}$$

where Rd is the radiation-conduction parameter or Plank number, θ_w is the surface heating parameter and Pr is the Prandtl number defined respectively as

$$Rd = \frac{4\sigma T_\infty^3}{k(\alpha_r + \sigma_s)} \quad \text{and} \quad Pr = \frac{\mu C_p}{k} \tag{3.11}$$

To solve equations (3.8)-(3.9), subject to the boundary conditions (3.10), we assume the following variables

$$\psi = \xi\, r(\xi) f(\xi,\eta), \quad \theta = \theta(\xi,\eta) \tag{3.12}$$

where ψ is the non-dimensional stream function defined in the usual way as

$$u = \frac{1}{r}\frac{\partial\psi}{\partial\eta}, \quad v = -\frac{1}{r}\frac{\partial\psi}{\partial\xi} \tag{3.13}$$

Substituting (3.13) into equations (3.8)-(3.9), after some algebra the following transformed equations take the following form

$$\frac{\partial^3 f}{\partial\eta^3} + \left(1 + \frac{\xi}{\sin\xi}\cos\xi\right) f \frac{\partial^2 f}{\partial\eta^2} - \left(\frac{\partial f}{\partial\eta}\right)^2 + \frac{\sin\xi}{\xi}\theta = \xi\left(\frac{\partial f}{\partial\eta}\frac{\partial^2 f}{\partial\xi\partial\eta} - \frac{\partial f}{\partial\xi}\frac{\partial^2 f}{\partial\eta^2}\right) \tag{3.14}$$

$$\frac{1}{\Pr}\frac{\partial}{\partial\eta}\left[\left\{1 + \frac{4}{3}Rd(1+\Delta\theta)^3\right\}\frac{\partial\theta}{\partial\eta}\right] + \left(1 + \frac{\xi}{\sin\xi}\cos\xi\right) f \frac{\partial\theta}{\partial\eta} = \xi\left(\frac{\partial f}{\partial\eta}\frac{\partial\theta}{\partial\xi} - \frac{\partial\theta}{\partial\eta}\frac{\partial f}{\partial\xi}\right) \tag{3.15}$$

Where $\Delta = \dfrac{a q_w / k}{T_\infty}$.

Along with boundary conditions

$$\begin{aligned} & f = \frac{\partial f}{\partial\eta} = 0, \ \ \theta' = -1 \ \text{ at } \ \eta = 0 \\ & \frac{\partial f}{\partial\eta} \to 0, \ \ \theta \to 0 \ \text{ as } \ \eta \to \infty \end{aligned} \tag{3.16}$$

It can be seen that near the lower stagnation point of the sphere i.e. $\xi \approx 0$, equations (3.14) and (3.15) reduce to the following ordinary differential equations:

$$f''' + 2ff'' - f'^2 + \theta = 0 \tag{3.17}$$

$$\frac{1}{\Pr}\left[\left\{1 + \frac{4}{3}Rd(1+\Delta\theta)^3\right\}\theta'\right]' + 2f\theta' = 0 \tag{3.18}$$

Subject to the boundary conditions

$$\begin{aligned} & f(0) = f'(0) = 0, \ \ \theta'(0) = -1 \\ & f' \to 0, \ \ \theta \to 0 \ \text{ as } \ \eta \to \infty \end{aligned} \tag{3.19}$$

In the above equations primes denote differentiation with respect to η.

In practical applications, the physical quantities of principle interest are the shearing stress, the rate heat transfer and the rate of species concentration transfer in terms of the skin-friction coefficients C_f and Nusselt number Nu_x respectively, which can be written as

$$C_f=\frac{(\tau_w)_{y=0}}{\rho U^2} \quad \text{and} \quad Nu=\frac{a q_w/k}{(T_w-T_\infty)} \tag{3.20}$$

$$\text{where} \quad \tau_w=\mu\left(\frac{\partial u}{\partial y}\right)_{y=0} \quad \text{and} \quad q_w=-k\left(\frac{\partial T}{\partial y}\right)_{y=0} \tag{3.21}$$

Here we have used a reference velocity $U=\frac{\nu Gr^{1/4}}{a}$

Using the variables (3.6) and (3.13) and the boundary condition (3.19) into (3.20)-(3.21), we get

$$C_f Gr^{-1/4}=\xi f''(\xi,0) \tag{3.22}$$

$$Nu Gr^{-1/4}=1/\theta(\xi,0) \tag{3.23}$$

The values of the velocity and temperature distribution are calculated respectively from the following relations:

$$u=\frac{\partial f}{\partial \eta}, \quad \theta=\theta(\xi,\eta) \tag{3.24}$$

3.3. Results and discussion

In this chapter we have been investigated the effects of radiation on natural convection flow with uniform heat flux on a sphere for different values of relevant physical parameters. For this we obtained the solutions for fluids having Prandtl number Pr = 0.72 (air) and for some test values of Pr = 1.0, 1.74, 2.0, 3.0 against η for a wide range of values of radiation parameter Rd. The values of radiation parameter Rd =1.0, 2.0, 3.0, 4.0 and 5.0 have been taken while Pr = 1.0 and Δ=0.1. Different values of surface temperature parameter Δ= 0.1, 0.2, 0.3, 0.4 and 0.5 are considered while Pr = 1.0 and Rd =1.0. We calculated the numerical values of local rate of heat transfer in terms of Nusselt number Nu for the surface of the sphere from lower stagnation point to upper stagnation point. The effect for different values of radiation parameter Rd on local skin friction coefficient C_f and the local Nusselt number Nu, as well as velocity and temperature profiles with the Prandtl number Pr = 1.0 and surface temperature parameter Δ= 0.1 are discussed.

By the displaying figures 3.2-3.3 we get the results for the velocity and temperature profiles, for different values of radiation parameter Rd while Prandtl number Pr = 1.0 and surface temperature parameter Δ= 0.1. From figures 3.2 and 3.3 we have seen that as the radiation parameter Rd increases both the velocity and the temperature increase. The changes of velocity profiles in the η direction reveals the typical velocity profile for natural convection boundary layer flow i.e. the velocity is zero at the boundary wall then the velocity increases to the peak value as ηincreases and finally the velocity approaches to zero (the asymptotic value). The maximum values of velocity are recorded to be 0.45896, 0.51374, 0.550830, 0.57840 and 0.60017 for Rd=1.0, 2.0, 3.0, 4.0 and 5.0 respectively which occur in between the points η = 1.23788 and η=1.43822. Here, it observed that at η = 1.36929, the velocity increases by 5.005%. The changes of temperature profiles in the η direction also shows the typical velocity profile for natural convection boundary layer flow that is the valne of temperature is 1.0 (one) at the boundary wall then the temperature decreases gradually along η direction to the asymptotic value.

Again the variation of the surface temperature parameter θ_w, the velocity and temperature profiles while Prandtl number Pr = 1.0 and radiation-conduction parameter Rd =1.0 are shown in the figures 3.4 and 3.5. Where. surface temperature parameter Δ increases, the velocity profile and the temperature increase but velocity increases near the surface of the sphere and then temperature decreases slowly and finally approaches to zero. Moreover, in the figures 3.6 and 3.7, when the Prandtl number Pr = 0.72, 1,0, 1.74, 2.0 and 3.0 increase with Δ= 0.1 and Rd =1.0 the velocity increase but the temperature decrease.

Figures 3.8-3.9 show that skin friction coefficient C_f and heat transfer coefficient Nu increase for increasing values of radiation parameter Rd, while Prandtl number Pr = 1.0 and surface temperature parameter Δ= 0.1. The values of skin friction C_f and Nusselt number Nu are recorded to be 1.04809, 1.11326, 1.15486, 1.18458, 1.20726 and .73750, .98790, 1.19677, 1.37972, 1.54469 for Rd=1.0, 2.0, 3.0, 4.0 and5.0 respectively which occur at the same point ξ = 1.57080. Here, it is observed that at ξ = 1.57080, the skin friction increases by 15.19 % and Nusselt number Nu increases by 1.09%. It is observed from the figure 3.8 that the skin friction increase gradually from zero value at lower stagnation point along the ξ direction and from figure 3.9, it reveals that the rate of heat transfer increase slightly along the ξ direction from lower stagnation point to the downstream.

It can also be seen from figures 3.10 - 3.11, that an increase in the surface temperature parameter Δ leads to increase the local skin friction coefficient C_f and the local rate of heat transfer Nu slightly while Prandtl number Pr = 1.0 and radiation parameter Rd =1.0. Also it is observed that at any position of ξ, the skin friction coefficient C_f and the local Nusselt number Nu increase as Δ increases from 0.1 to 0.5. This phenomenon can easily be understood from the fact that when the surface temperature parameter Δ increase. the temperature of the fluid rises and the thickness of the velocity of the boundary layer grows i.e. the thermal boundary layer becomes thinner than the velocity at the boundary layer. Therefore the skin friction coefficient C_f and the local Nusselt number Nu increase.

Variations of the local skin friction coefficient C_f and local rate of heat transfer Nu for different values of Prandtl number Pr while Δ = 0.1 and Rd =1.0 are shown in the figures 3.12 and 3.13. We can observe from the figures that as the Prandtl number Pr increases, the skin friction coefficient decreases and heat transfer coefficient increases but the rate of increase in the heat transfer coefficient is higher than that of the skin friction coefficient. So, the effect of Prandtl number Pr on heat transfer coefficient is more than of the effect of Pr on skin friction coefficient.

The numerical values of skin friction coefficient C_f and rate of heat transfer Nu are calculated from equations (3.22) and (3.23) for the surface of the sphere from lower stagnation point to upper stagnation point. Numerical values of C_f and Nu are depicted in Table 3.1, Table 3.2 and in Table 3.3.

Table 3. 1: Skin friction coefficient and rate of heat transfer against ξ for different values of Prandtl numbers and against fixed radiation numbers Rd = 1.0 and Δ=0.1.

	Pr = 0.72		Pr = 1.00		Pr = 1.74		Pr = 3.00	
ξ	C_f	Nu	C_f	Nu	C_f	Nu	C_f	Nu
0.00000	0.00000	0.77199	0.00000	0.87801	0.00000	1.07981	0.00000	1.30932
0.10472	0.09626	0.77142	0.09235	0.87735	0.08544	1.07900	0.07843	1.30834
0.20944	0.19184	0.76978	0.18405	0.87549	0.17027	1.07671	0.15631	1.30556
0.31416	0.28609	0.76709	0.27447	0.87242	0.25393	1.07294	0.23311	1.30099
0.40143	0.36314	0.76403	0.34839	0.86894	0.32231	1.06866	0.29589	1.29580
0.50615	0.45325	0.75939	0.43485	0.86365	0.40230	1.06214	0.36932	1.28791
0.61087	0.54022	0.75367	0.51829	0.85714	0.47950	1.05413	0.44019	1.27819
0.71558	0.62343	0.74686	0.59812	0.84939	0.55337	1.04459	0.50800	1.26664
0.80285	0.68946	0.74036	0.66149	0.84198	0.61199	1.03548	0.56182	1.25559
0.90757	0.76425	0.73154	0.73324	0.83193	0.67839	1.02311	0.62278	1.24060
1.01229	0.83365	0.72159	0.79984	0.82061	0.74001	1.00918	0.67935	1.22371
1.20428	0.94516	0.70039	0.90686	0.79646	0.83904	0.97946	0.77027	1.18769
1.30900	0.99652	0.68716	0.95616	0.78138	0.88467	0.96090	0.81216	1.16519
1.46608	1.05983	0.66502	1.01693	0.75614	0.94092	0.92985	0.86381	1.12755
1.57080	1.09227	0.64866	1.04809	0.73750	0.96976	0.90691	0.89029	1.09974

Table 3.2: Skin friction coefficient and rate of heat transfer against ξ for different values of radiation parameter against fixed Prandtl number Pr = 1.0 and Δ=0.1.

	Rd = 1.00		Rd = 2.00		Rd = 3.00		Rd=5.00	
ξ	C_f	Nu	C_f	Nu	C_f	Nu	C_f	Nu
0.00000	0.00000	0.87801	0.00000	1.17558	0.00000	1.42388	0.00000	1.83752
0.10472	0.09235	0.87735	0.09811	1.17470	0.10178	1.42282	0.10639	1.83614
0.20944	0.18405	0.87549	0.19553	1.17221	0.20283	1.41981	0.21203	1.83226
0.31416	0.27447	0.87242	0.29159	1.16811	0.30248	1.41485	0.31619	1.82586
0.40143	0.34839	0.86894	0.37012	1.16346	0.38394	1.40922	0.40134	1.81860
0.50615	0.43485	0.86365	0.46196	1.15639	0.47922	1.40066	0.50094	1.80757
0.61087	0.51829	0.85714	0.55060	1.14769	0.57117	1.39012	0.59706	1.79398
0.71558	0.59812	0.84939	0.63541	1.13733	0.65914	1.37759	0.68902	1.77782
0.80285	0.66149	0.84198	0.70271	1.12743	0.72896	1.36561	0.76201	1.76237
0.90757	0.73324	0.83193	0.77893	1.11401	0.80803	1.34937	0.84466	1.74142
1.01229	0.79984	0.82061	0.84967	1.09888	0.88141	1.33106	0.92137	1.71782
1.20428	0.90686	0.79646	0.96332	1.06662	0.99931	1.29202	1.04463	1.66748
1.30900	0.95616	0.78138	1.01567	1.04648	0.05362	1.26765	1.10141	1.63606
1.46608	1.01693	0.75614	1.08019	1.01279	1.12056	1.22688	1.17139	1.58350
1.57080	1.04809	0.73750	1.11326	0.98790	1.15486	1.19677	1.20726	1.54469

Table 3. 3: Skin friction coefficient and rate of heat transfer against ξ for different values of ∇, against fixed radiation numbers Rd = 1.0 and Pr = 1.0.

	$\Delta = 0.1$		$\Delta = 0.2$		$\Delta = 0.4$		$\Delta = 0.5$	
ξ	C_f	Nu	C_f	Nu	C_f	Nu	C_f	Nu
0.00000	0.00000	0.87751	0 00000	0.94408	0.00000	1.09305	0.00000	1.17454
0 10472	0.09237	0.87685	0.09417	0.94337	0.09767	1.09223	0.09936	1.17366
0 20944	0.18409	0.87499	0.18767	0 94137	0.19465	1.08992	0.19801	1.17117
0.31416	0.27452	0.87193	0.27986	0 93807	0.29028	1.08610	0.29529	1.16706
0.40143	0.34846	0.86845	0.35524	0.93433	0.36846	1.08177	0.37482	1.16241
0 50615	0.43493	0.86315	0.44340	0.92864	0.45990	1.07518	0 46783	1.15533
0 61087	0.51839	0.85664	0.52848	0.92163	0.54815	1.06707	0.55760	1.14661
0 71558	0.59824	0.84889	0.60988	0.91329	0.63258	1.05742	0.64349	1.13624
0 80285	0.66161	0.84148	0.67449	0.90532	0 69959	1.04819	0.71166	1.12633
0.90757	0.73338	0.83144	0.74766	0.89452	0 77549	1.03568	0.78887	1.11288
1.01229	0.79999	0.82012	0.81556	0.88234	0.84592	1.02159	0.86052	1.09773
1.20428	0.90703	0.79597	0.92468	0.85636	0.95910	0.99152	0.97566	1.06542
1.30900	0.95634	0.78089	0.97495	0.84014	1.01125	0.97274	1.02870	1.04525
1.46608	1.01713	0.75566	1.03693	0.81300	1 07553	0.94133	1.09409	1.01149
1.57080	1.04829	0.73703	1.06869	0.79295	1.10848	0.91812	1.12761	0.98655

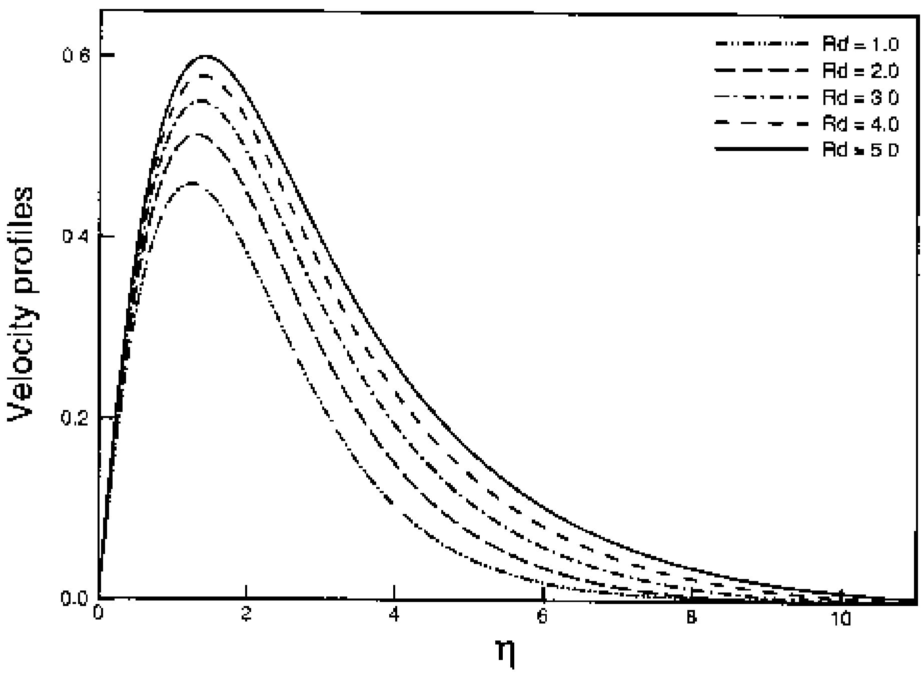

Figure 3.2: Velocity profiles for different values of Rd when Pr = 1.0 and $\Delta = 0.1$

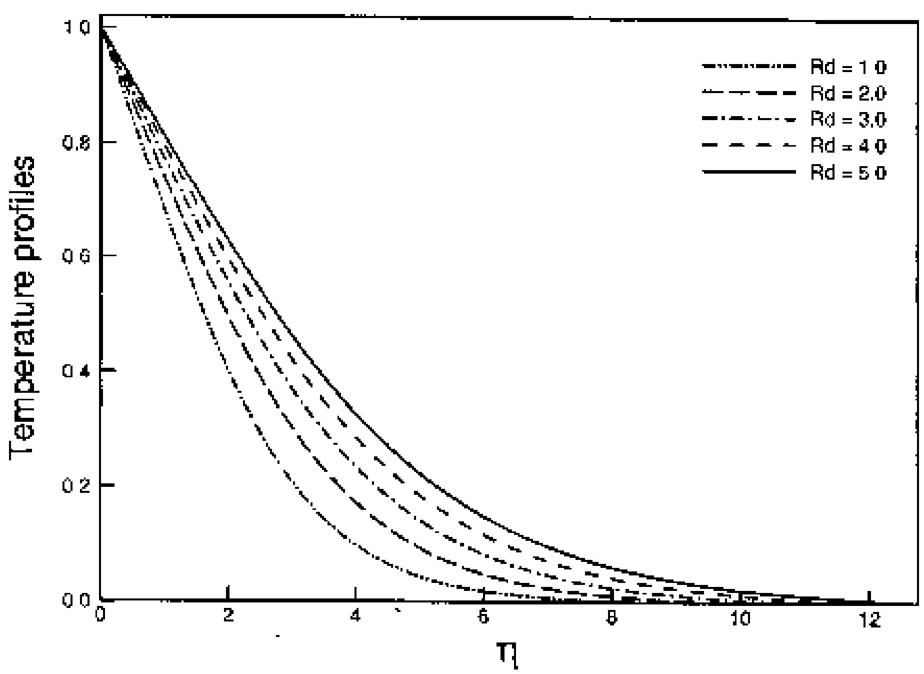

Figure 3.3: Temperature profiles for different values of Rd when Pr = 1.0 and $\Delta = 0.1$

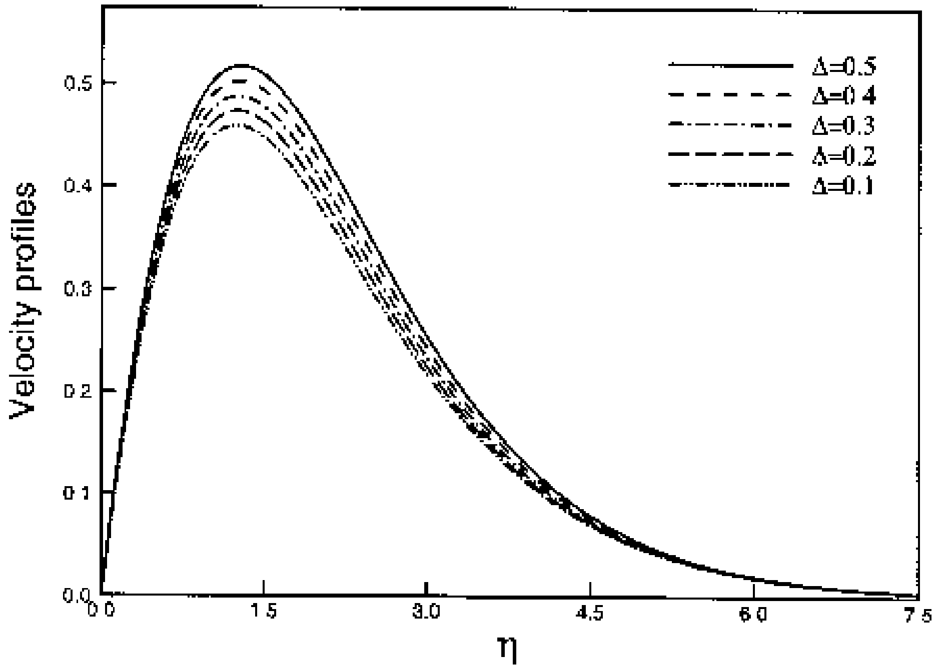

Figure 3.4: Velocity profiles for different values of Δ while Rd=1.0 and Pr = 1.0.

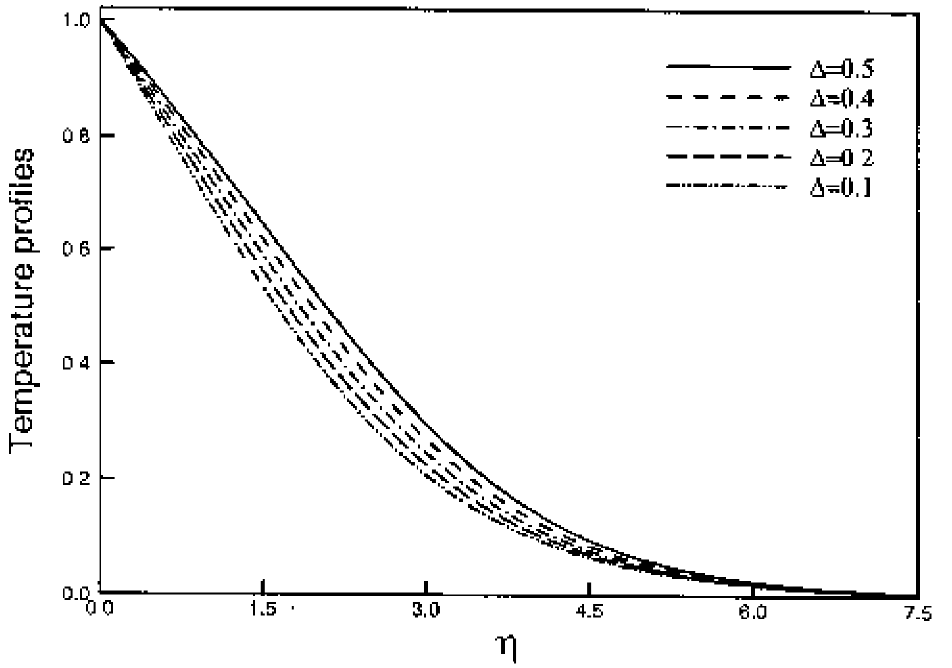

Figure 3.5: Temperature profiles for different values of Δ while Rd=1.0 and Pr = 1.0.

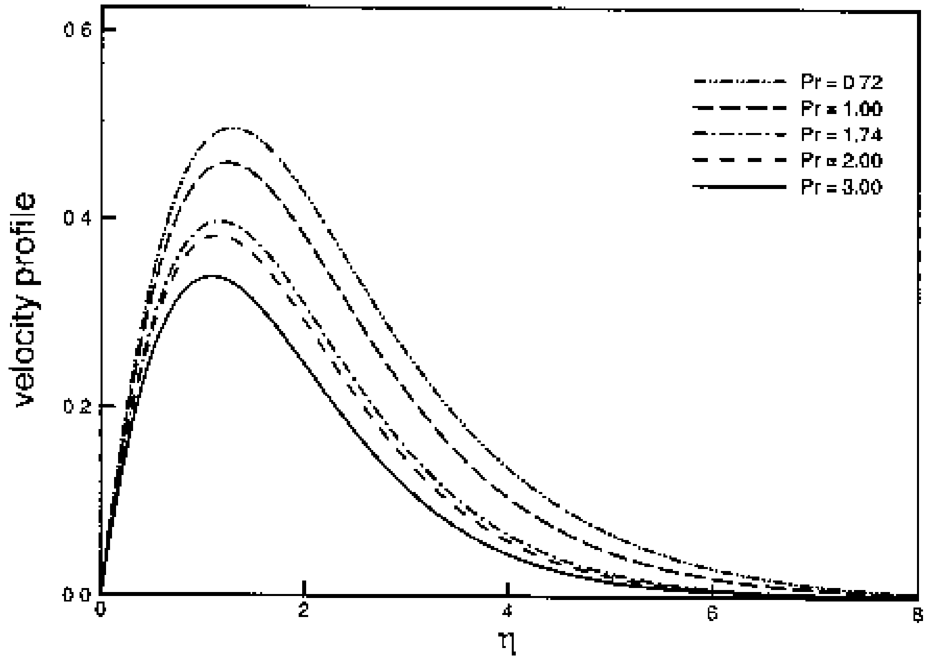

Figure 3.6: Velocity profiles for different values of Pr while Rd=1.0 and $\Delta = 0.1$.

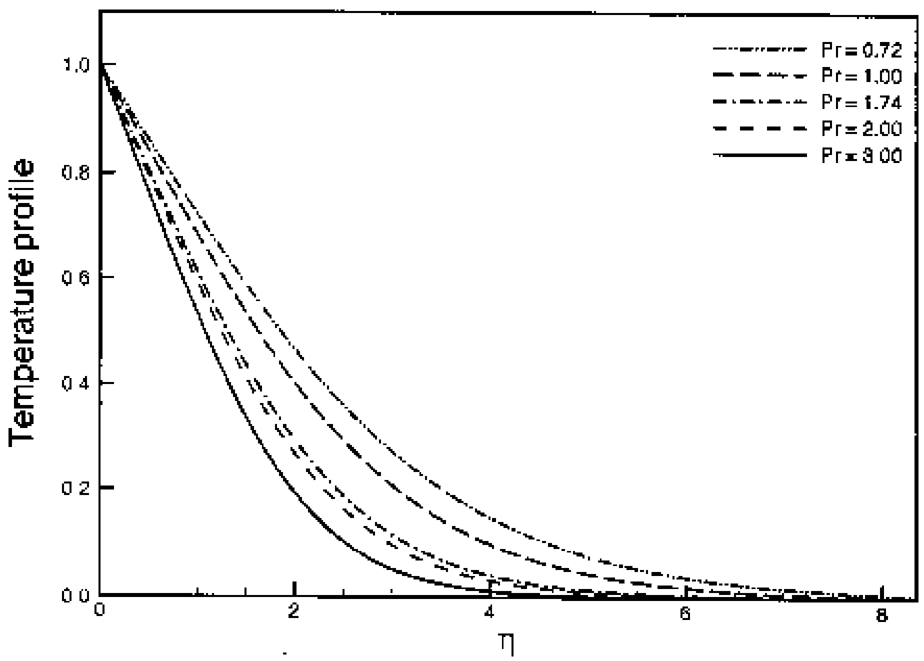

Figure 3.7: Temperature profiles for different values of Pr while Rd=1.0 and $\Delta = 0.1$.

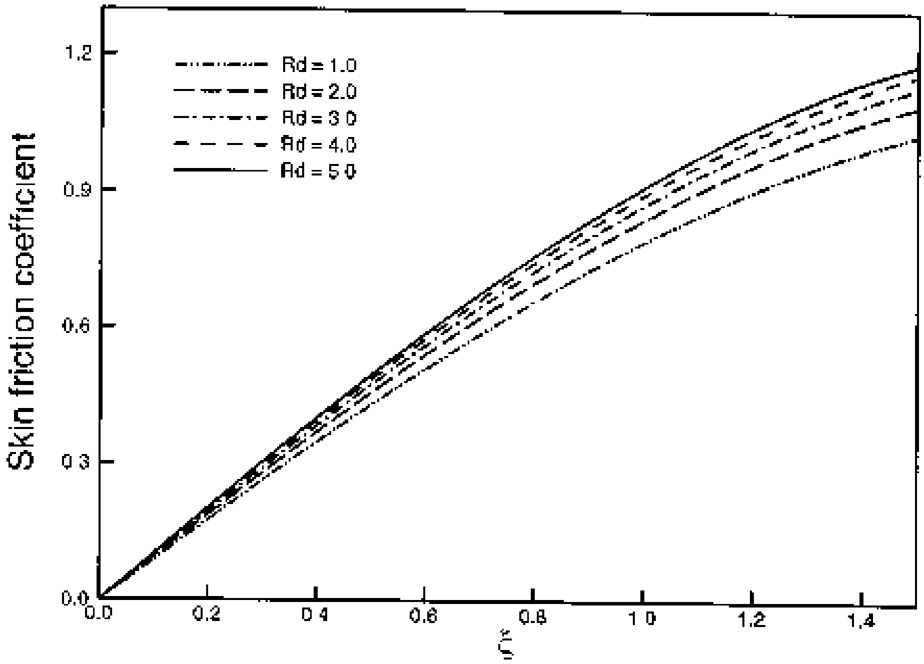

Figure 3.8: Skin friction coefficients for different values of Rd= while Pr =1.0 and $\Delta = 0.1$

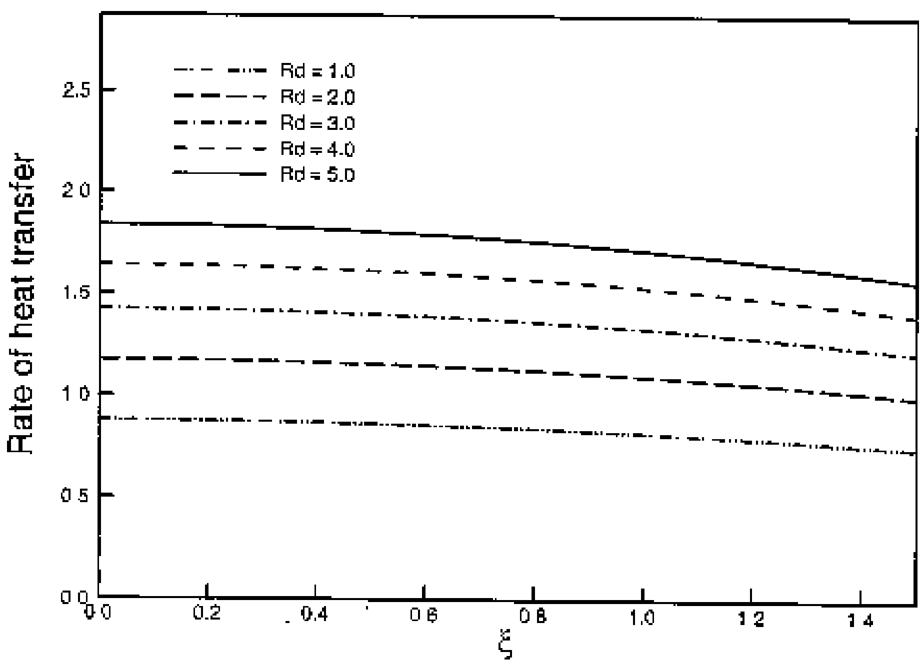

Figure 3.9: Heat transfer coefficients for different values of Rd while Pr=1.0 and $\Delta = 0.1$

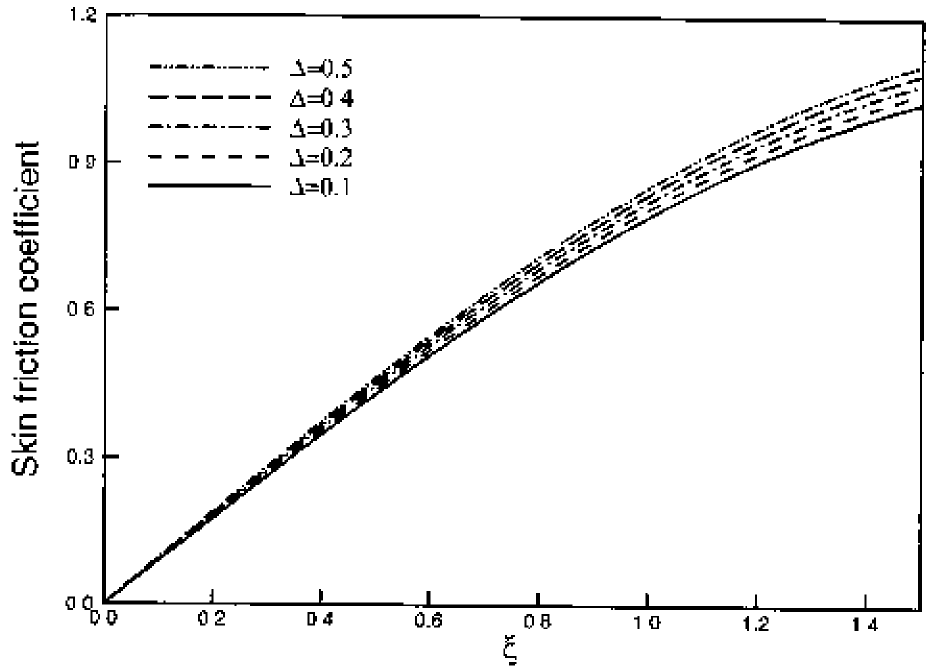

Figure 3.10: Skin friction coefficients for different values of Δ, while Rd = 1.0 and Pr =1.0

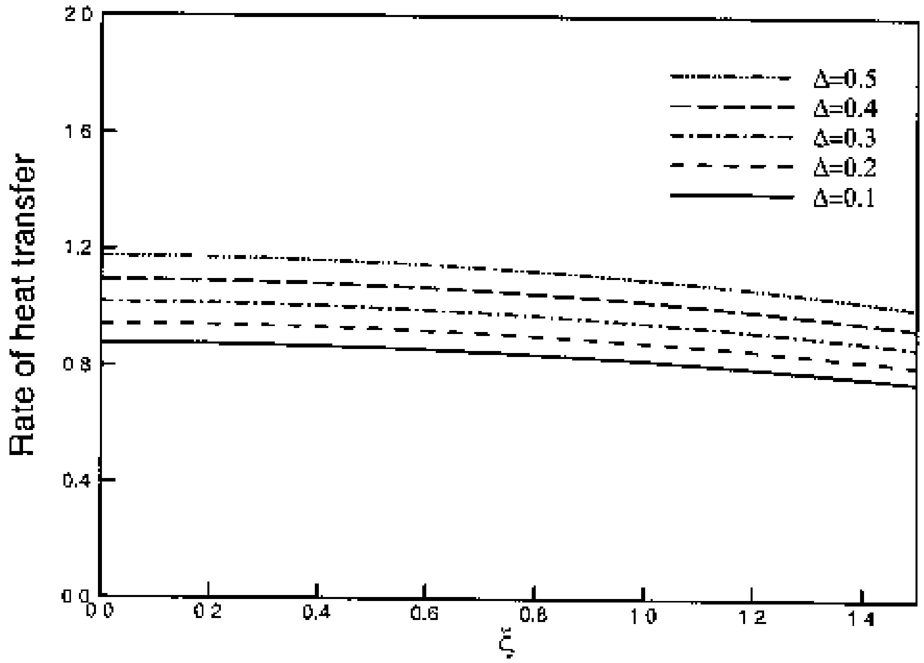

Figure 3.11: Heat transfer coefficients for different values of Δ, while Rd=1.0 and Pr =1.0.

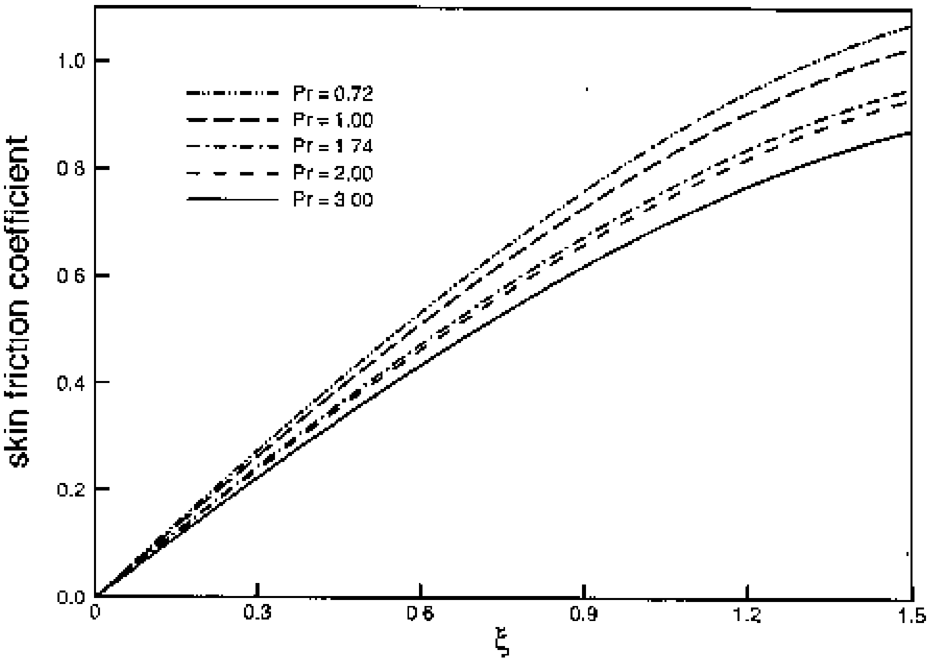

Figure 3.12: Skin friction coefficients for different values of Pr, while Rd = 1.0 and Δ = 0.1

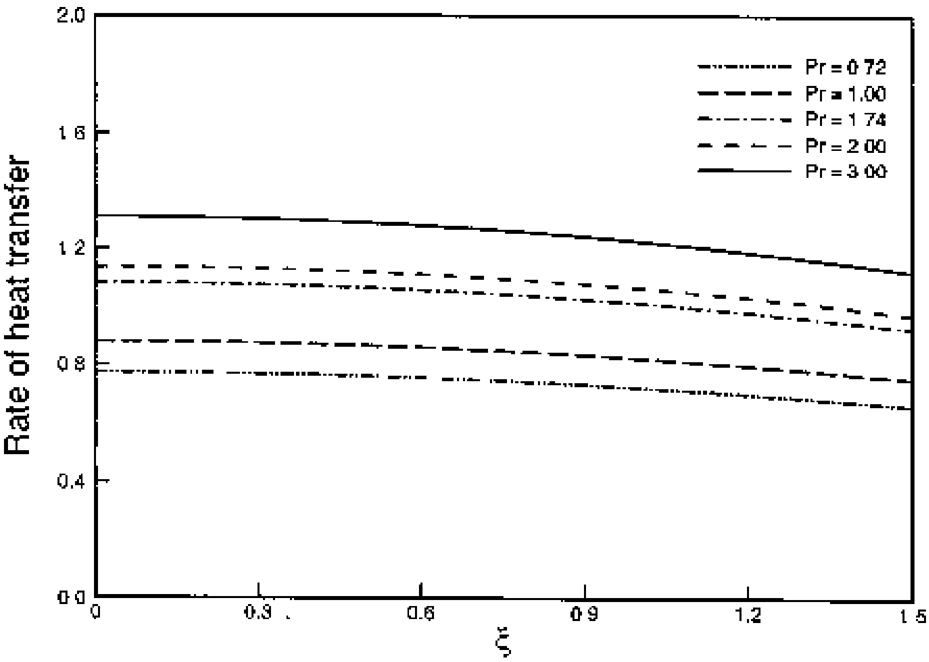

Figure 3.13: Heat transfer coefficients for different values of Pr While Rd = 1.0 and Δ = 0.1

3.4. Conclusion

The Radiation effect on natural convection flow on a sphere with uniform heat flux has been studied for different values of relevant physical parameters including Prandtl number Pr, and surface temperature parameter Δ.

In this work we have transformed the governing boundary layer equations of motion into a non-dimensional form and then the resulting non-linear systems of partial differential equations are reduced to local non-similarity boundary layer equations, which are solved numerically by using implicit finite difference method together with the Keller-box scheme. By the present investigation we can draw the following conclusions:

- There are significant effects of radiation parameter Rd on velocity and temperature profiles as well as on skin friction and the rate of heat transfer have been found in this study. An increase in the values of radiation parameter Rd leads to both the velocity and the temperature profiles increase, the local skin friction coefficient C_f and the local rate of heat transfer Nu also increases for increase of Rd at different position of ξ for Pr=1.0. and Δ=0.1.
- When the values of surface temperature parameter Δ increases while Rd=1.0 and Pr=1.0 then all the velocity profiles, temperature profiles, the local skin friction coefficients C_f and the local rate of heat transfer Nu increase significantly.
- Again for increasing values of Prandtl number Pr leads to decrease on the velocity and temperature profiles and the local skin friction coefficient C_f, but the local rate of heat transfer Nu increases as the increase of the Prandtl number while Rd=1.0 and Δ=0.1.

3.5 Extension of this work

In this work, we considered constant viscosity and thermal conductivity but they are functions of temperature.

- If we consider the viscosity and thermal conductivity as the function of temperature then we can extend our problem.
- We can extend the work by taking into account the MHD effect.
- Also taking the non-uniform surface temperature, the problem can be extended.

Appendix-A

Implicit Finite Difference Method

To get the solutions of the transformed governing equations with the corresponding boundary conditions. we employed implicit finite difference method together with Keller-box elimination technique, which is well documented and widely used by Keller and Cebeci (1971) and recently by Hossain et al. (1990, 1992, 1996, 1997, 1998).

A brief discussion on the development of algorithm on the method of implicit finite difference method together with Keller – box elimination scheme is given below considering the following Equations (A1-A2).

$$\frac{\partial^3 f}{\partial \eta^3}+\left(1+\frac{\xi}{\sin\xi}\cos\xi\right)f\frac{\partial^2 f}{\partial \eta^2}-\left(\frac{\partial f}{\partial \eta}\right)^2+\frac{\sin\xi}{\xi}\theta=\xi\left(\frac{\partial f}{\partial \eta}\frac{\partial^2 f}{\partial \xi\partial \eta}-\frac{\partial f}{\partial \xi}\frac{\partial^2 f}{\partial \eta^2}\right) \qquad \text{(A1)}$$

$$\frac{1}{\Pr}\frac{\partial}{\partial \eta}\left[\left\{1+\frac{4}{3}Rd\left(1+(\theta_w-1)\theta\right)^3\right\}\frac{\partial \theta}{\partial \eta}\right]+\left(1+\frac{\xi}{\sin\xi}\cos\xi\right)f\frac{\partial \theta}{\partial \eta} \qquad \text{(A2)}$$
$$=\xi\left(\frac{\partial f}{\partial \eta}\frac{\partial \theta}{\partial \xi}-\frac{\partial \theta}{\partial \eta}\frac{\partial f}{\partial \xi}\right)$$

To apply the aforementioned method, we first convert Equations (A1)-(A2) into the following system of first order equations with dependent variables $u\ (\xi,\eta)$, $v\ (\xi\ \eta)$, $p\ (\xi\ \eta)$, and $g\ (\xi\ \eta)$ as

$$f'=u \qquad \text{(A3)}$$

$$u'=v \qquad \text{(A4)}$$

$$g'=p \qquad \text{(A5)}$$

$$v'+p_1fv-p_2u^2+p_3g=\xi\left(u\frac{\partial u}{\partial \xi}-\frac{\partial f}{\partial \xi}v\right) \qquad \text{(A6)}$$

$$\frac{1}{\Pr}\left(1+\frac{4}{3}p_4\right)p'+\frac{4}{pr}p_4g^2p^2+p_1fp=\xi\left(u\frac{\partial g}{\partial\xi}-p\frac{\partial f}{\partial\xi}\right) \quad \text{(A7)}$$

Where $\xi = x$, $h = g$ and

$$p_1 = 1+\frac{\xi}{\sin\xi}\cos\xi\ ,\ p_2 = 1,\ p_3 = \frac{\sin\xi}{\xi}\ ,\ p_4 = Rd\{1+(\theta_w-1)\}^3 \quad \text{(A8)}$$

and the boundary conditions are

$$f(\xi, 0) = 0,\ u(\xi, 0) = 0 \text{ and } g(\xi, 0) = 1$$

$$u(\xi, \infty) = 0,\ g(\xi, \infty) = 0 \quad \text{(A9)}$$

We now consider the net rectangle on the (ξ, η) plane shown in the figure (A1) and denote the net points by

$$\xi^0 = 0,\quad \xi^n = \xi^{n-1}+k_n\ ,\quad n = 1,2,\ldots N \quad \text{(A10)}$$

$$\eta_0 = 0,\quad \eta_j = \eta_{j-1}+h_j,\qquad j = 1,2\ldots J$$

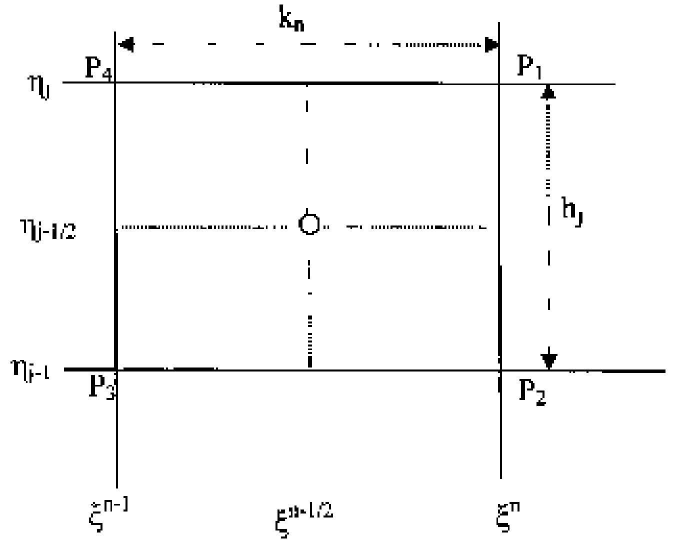

Figure A1: Net rectangle for difference approximations for the Box scheme.

Here 'n' and 'j' are just sequence of numbers on the (ξ, η) plane, k_n and h_j are the variable mesh widths.

We approximate the quantities f, u, v, p at the points (ξ^n, η_j) of the net by f^n_j, u^n_j, v^n_j, p^n_j which we call net function. We also employ the notation g^n_j for the quantities midway between net points shown in figure (3.14) and for any net function as

$$\xi^{n-1/2} = \frac{1}{2}(\xi^n + \xi^{n-1}) \tag{A11}$$

$$\eta_{j-1/2} = \frac{1}{2}(\eta_j + \eta_{j-1}) \tag{A12}$$

$$g_j^{n-1/2} = \frac{1}{2}(g_j^n + g_j^{n-1}) \tag{A13}$$

$$g^n_{j-1/2} = \frac{1}{2}(g_j^n + g^n_{j-1}) \tag{A14}$$

The finite difference approximations according to Box method to the three first order ordinary differential equations (A3)-(A5) are written for the mid point $(\xi^n, \eta_{j-1/2})$ of the segment P_1P_2 shown in the figure (3.14) and the finite difference approximations to the two first order differential equations (A6)-(A7) are written for the mid point $(\xi^{n-1/2}, \eta_{j-1/2})$ of the rectangle $P_1P_2P_3P_4$. This procedure yields.

$$h_j^{-1}(f_j^n - f_{j-1}^n) = u^n_{j-1/2} = \frac{u^n_{j-1} + u^n_j}{2} \tag{A15}$$

$$h_j^{-1}(u_j^n - u_{j-1}^n) = v^n_{j-1/2} = \frac{v^n_{j-1} + v^n_j}{2} \tag{A16}$$

$$h_j^{-1}(g_j^n - g_{j-1}^n) = p^n_{j-1/2} = \frac{p^n_{j-1} - p^n_j}{2} \tag{A17}$$

$$\frac{1}{2}\left(\frac{v_j^n - v_{j-1}^n}{h_j} + \frac{v_j^{n-1} - v_{j-1}^{n-1}}{h_j}\right) + (p_1 fv)^{n-1/2}_{j-1/2} - (p_2 u^2)^{n-1/2}_{j-1/2} + (p_3 g)^{n-1/2}_{j-1/2}$$
$$= \xi^{n-1/2}_{j-1/2}\left(u^{n-1/2}_{j-1/2}\,\frac{u^n_{j-1/2} - u^{n-1}_{j-1/2}}{k_n} - v^{n-1/2}_{j-1/2}\,\frac{f^n_{j-1/2} - f^{n-1}_{j-1/2}}{k_n}\right) \tag{A18}$$

$$\frac{1}{2P_r}\left(1+\frac{4}{3}p_4\right)\left(\frac{p_j^n - p_{j-1}^n}{h_j}+\frac{p_j^{n-1} - p_{j-1}^{n-1}}{h_j}\right)+(p_1 fp)_{j-1/2}^{n-1/2}+\frac{4}{P_r}(p_4(gp)^2)_{j-1/2}^{n-1/2}$$
$$=\xi_{j-1/2}^{n-1/2}\left(u_{j-1/2}^{n-1/2}\frac{g_{j-1/2}^n - g_{j-1/2}^{n-1}}{k_n}-p_{j-1/2}^{n-1/2}\frac{f_{j-1/2}^n - f_{j-1/2}^{n-1}}{k_n}\right) \qquad \text{(A19)}$$

Now from the equation (A18) we get

$$\frac{1}{2}\left(\frac{v_j^n - v_{j-1}^n}{h_j}\right)+\frac{1}{2}\left(\frac{v_j^{n-1} - v_{j-1}^{n-1}}{h_j}\right)+\frac{1}{2}\left\{(p_1 fv)_{j-1/2}^n+(p_1 fv)_{j-1/2}^{n-1}\right\}$$
$$-\frac{1}{2}\left\{(p_2 u^2)_{j-1/2}^n+(p_2 u^2)_{j-1/2}^{n-1}\right\}+\frac{1}{2}\left\{(p_3 g)_{j-1/2}^n+(p_3 g)_{j-1/2}^{n-1}\right\}$$
$$=\frac{1}{2k_n}\xi_{j-1/2}^{n-1/2}(u_{j-1/2}^n+u_{j-1/2}^{n-1})(u_{j-1/2}^n-u_{j-1/2}^{n-1})$$
$$-\frac{1}{2k_n}\xi_{j-1/2}^{n-1/2}(v_{j-1/2}^{n-1/2}+v_{j-1/2}^{n-1/2})(f_{j-1/2}^n-f_{j-1/2}^{n-1})$$

$$\Rightarrow h_j^{-1}(v_j^n-v_{j-1}^n)+h_j^{-1}(v_j^{n-1}-v_{j-1}^{n-1})+(p_1)_{j-1/2}^n(fv)_{j-1/2}^n$$
$$+(p_1)_{j-1/2}^{n-1}(fv)_{j-1/2}^{n-1}-(p_2)_{j-1/2}^n(u^2)_{j-1/2}^n-(p_2)_{j-1/2}^{n-1}$$
$$(u^2)_{j-1/2}^{n-1}+(p_3)_{j-1/2}^n(g)_{j-1/2}^n+(p_3)_{j-1/2}^{n-1}(g)_{j-1/2}^{n-1}$$
$$=\alpha_n\{(u^2)_{j-1/2}^n-(fv)_{j-1/2}^n+v_{j-1/2}^n f_{j-1/2}^{n-1}-v_{j-1/2}^{n-1}f_{j-1/2}^n+(fv)_{j-1/2}^{n-1}\}$$

$$\Rightarrow h_j^{-1}(v_j^n-v_{j-1}^n)+\left\{(p_1)_{j-1/2}^n+\alpha_n\right\}(fv)_{j-1/2}^n-\left\{(p_2)_{j-1/2}^n+\alpha_n\right\}$$
$$(u^2)_{j-1/2}^n+(p_3)_{j-1/2}^n(g)_{j-1/2}^n=\alpha_n\{-(u^2)_{j-1/2}^{n-1}+v_{j-1/2}^n f_{j-1/2}^{n-1}-v_{j-1/2}^{n-1}f_{j-1/2}^{n1}$$
$$+(fv)_{j-1/2}^{n-1}\}-(p_1)_{j-1/2}^{n-1}(fv)_{j-1/2}^{n-1}+(p_2)_{j-1/2}^{n-1}(u^2)_{j-1/2}^{n-1}$$
$$-(p_3)_{j-1/2}^n(g)_{j-1/2}^n-h_j^{-1}(v_j^{n-1}-v_{j-1}^{n-1})\}$$
$$\Rightarrow h_j^{-1}(v_j^n-v_{j-1}^n)+\left\{(p_1)_{j-1/2}^n+\alpha_n\right\}(fv)_{j-1/2}^n-\left\{(p_2)_{j-1/2}^n+\alpha_n\right\}(u^2)_{j-1/2}^n$$
$$+(p_3)_{j-1/2}^n(g)_{j-1/2}^n=\alpha_n\{-(u^2)_{j-1/2}^{n-1}+(fv)_{j-1/2}^{n-1}+v_{j-1/2}^{n-1}f_{j-1/2}^n$$
$$-v_{j-1/2}^n f_{j-1/2}^{n-1})\}-(p_1)_{j-1/2}^{n-1}(fv)_{j-1/2}^{n-1}+(p_2)_{j-1/2}^{n-1}(u^2)_{j-1/2}^{n-1}$$
$$-h_j^{-1}(v_j^{n-1}-v_{j-1}^{n-1})+(p_3)_{j-1/2}^{n-1}(g)_{j-1/2}^{n-1}$$

$$\Rightarrow h_j^{-1}(v_j^n - v_{j-1}^n) + \left\{(p_1)_{j-1/2}^n + \alpha_n\right\}(fv)_{j-1/2}^n - \left\{(p_2)_{j-1/2}^n + \alpha_n\right\}$$

$$(u^2)_{j-1/2}^n + (p_3)_{j-1/2}^n (g)_{j-1/2}^n + \alpha_n (v_{j-1/2}^{n-1} f_{j-1/2}^n - v_{j-1/2}^n f_{j-1/2}^{n-1})$$

$$= -L_{j-1/2}^n + \alpha_n \left\{(fv)_{j-1/2}^{n-1} - (u^2)_{j-1/2}^{n-1}\right\}$$

$$L_{j-1/2}^{n-1} = (p_1)_{j-1/2}^{n-1}(fv)_{j-1/2}^{n-1} - (p_2)_{j-1/2}^{n-1}(u^2)_{j-1/2}^{n-1}$$

$$+ \quad h_j^{-1}(v_j^{n-1} - v_{j-1}^{n-1}) - (p_3)_{j-1/2}^{n-1}(g)_{j-1/2}^{n-1}$$

$$\Rightarrow h_j^{-1}(v_j^n - v_{j-1}^n) + \left\{(p_1)_{j-1/2}^n + \alpha_n\right\}(fv)_{j-1/2}^n - \left\{(p_2)_{j-1/2}^n + \alpha_n\right\}$$

$$(u^2)_{j-1/2}^n + (p_3)_{j-1/2}^n (g)_{j-1/2}^n + \alpha_n (v_{j-1/2}^{n-1} f_{j-1/2}^n \qquad \text{(A20)}$$

$$-v_{j-1/2}^n f_{j-1/2}^{n-1}) = R_{j-1/2}^{n-1}$$

$$\text{where} \quad R_{j-1/2}^{n-1} = -L_{j-1/2}^n + \alpha_n \left\{(fv)_{j-1/2}^{n-1} - (u^2)_{j-1/2}^{n-1}\right\}$$

Again from the equation (A19) we get

$$\frac{1}{P_r}\left(1 + \frac{4}{3}p_4\right) h_j^{-1}(p_j^n - p_{j-1}^n) + \left\{(p_1)_{j-1/2}^{n-1/2} + \alpha_n\right\}(fp)_{j-1/2}^n$$

$$+\frac{4}{P_r}\left\{(p_4)_{j-1/2}^n ((gp)^2)_{j-1/2}^n\right\} + \alpha_n (u_{j-1/2}^n g_{j-1/2}^{n-1} - u_{j-1/2}^{n-1} g_{j-1/2}^n$$

$$-p_{j-1/2}^n f_{j-1/2}^{n-1} + p_{j-1/2}^{n-1} f_{j-1/2}^n) = -M_{j-1/2}^{n-1} - \alpha_n \left\{(fp)_{j-1/2}^{n-1} - (ug)_{j-1/2}^{n-1}\right\}$$

$$\text{where} \quad M_{j-1/2}^{n-1} = \frac{1}{P_r} h_j^{-1}\left(1 + \frac{4}{3}p_4\right)(p_j^{n-1} - p_{j-1}^{n-1}) + (p_1)_{j-1/2}^{n-1/2}(fp)_{j-1/2}^{n-1}$$

$$-\frac{4}{P_r}(p_4)_{j-1/2}^{n-1/2}((gp)^2)_{j-1/2}^{n-1}$$

$$\Rightarrow \frac{1}{P_r}\left(1+\frac{4}{3}p_4\right)h_j^{-1}(p_j^n - p_{j-1}^n)+\left\{(p_1)_{j-1/2}^{n-1/2}+\alpha_n\right\}(fp)_{j-1/2}^n$$

$$+\frac{4}{p_r}\left\{(p_4)_{j-1/2}^n((gp)^2)_{j-1/2}^n\right\}+\alpha_n(u_{j-1/2}^n g_{j-1/2}^{n-1} \tag{A21}$$

$$-u_{j-1/2}^{n-1}g_{j-1/2}^n - p_{j-1/2}^n f_{j-1/2}^{n-1} + p_{j-1/2}^{n-1} f_{j-1/2}^n) = T_{j-1/2}^{n-1}$$

$$where \quad T_{j-1/2}^{n-1} = -M_{j-1/2}^{n-1} + \alpha_n\left\{(fp)_{j-1/2}^{n-1} - (ug)_{j-1/2}^{n-1}\right\}$$

The boundary conditions become

$$f_0^n = 0 \quad u_0^n = 0 \quad p_0^n = 1$$
$$u_J^n = 0 \quad g_J^n = 0 \tag{A22}$$

If we assume $f_j^{n-1}, u_j^{n-1}, v_j^{n-1}, g_j^{n-1}, p_j^{n-1}$ to be known for $0 \le j \le J$, equations (A15) to (A17) and (A20) – (A21) form a system of $5J + 5$ non linear equations for the solutions of the $5J + 5$ unknowns ($f_j^n, u_j^n, v_j^n, g_j^n, p_j^n$) , j = 0,1,2 ...J. These non-linear systems of algebric equations are to be linearized by Newton's Quassy linearization method. We define the iterates [$f_j^n, u_j^n, v_j^n, g_j^n, p_j^n$] , i = 0,1,2 ...N with initial values equal those at the previous x-station (which is usually the best initial available) . For the higher iterates we set

$$f_j^{(i+1)} = f_j^{(i)} + \delta f_j^{(i)} \tag{A23}$$
$$u_j^{(i+1)} = u_j^{(i)} + \delta u_j^{(i)} \tag{A24}$$
$$v_j^{(i+1)} = v_j^{(i)} + \delta v_j^{(i)} \tag{A25}$$
$$g_j^{(i+1)} = g_j^{(i)} + \delta g_j^{(i)} \tag{A26}$$
$$p_j^{(i+1)} = p_j^{(i)} + \delta p_j^{(i)} \tag{A27}$$

Now by substituting the right hand sides of the above eqnations in place of f_j^n, u_j^n, v_j^n and g_j^n omitting the terms that are quadratic in δf_j^i , $\delta u_j^i, \delta v_j^i$, δp_j^i we get the equations (A15) ,(A16)and (A17) in the following form:

$$f_j^{(i)} + \delta f_j^{(i)} - f_{j-1}^{(i)} - \delta f_{j-1}^{(i)} = \frac{h_j}{2}\left\{u_j^{(i)} + \delta u_j^{(i)} + u_{j-1}^{(i)} + \delta u_{j-1}^{(i)}\right\}$$

$$\delta f_j^{(i)} - \delta f_{j-1}^{(i)} - \frac{h_j}{2}(\delta u_j^{(i)} + \delta u_{j-1}^{(i)}) = (r_1)_j \tag{A28}$$

Where $(r_1)_j = f_{j-1}^{(i)} - f_j^{(i)} + h_j u_{j-1/2}^{(i)}$ (A29)

$$\delta u_j^{(i)} - \delta u_{j-1}^{(i)} - \frac{h_j}{2}(\delta v_j^{(i)} + \delta v_{j-1}^{(i)}) = (r_4)_j \tag{A30}$$

$$(r_4)_j = u_{j-1}^{(i)} - u_j^{(i)} + h_j v_{j-1/2}^{(i)} \tag{A31}$$

$$\delta g_j^{(i)} - \delta g_{j-1}^{(i)} - \frac{h_j}{2}(\delta p_j^{(i)} + \delta p_{j-1}^{(i)}) = (r_5)_j \tag{A32}$$

Where $(r_5)_j = g_{j-1}^{(i)} - g_j^{(i)} + h_j p_{j-1/2}^{(i)}$ (A33)

Now the moment of equation becomes:

$$h_j^{-1}(v_j^{(i)} + \delta v_j^{(i)} - v_{j-1}^{(i)} - \delta v_{j-1}^{(i)}) + \left\{(p_1)_{j-1/2}^n + \alpha_n\right\}\left\{(fv)_{j-1/2}^{(i)} + \delta(fv)_{j-1/2}^{(i)}\right\}$$

$$-\left\{(p_2)_{j-1/2}^n + \alpha_n\right\}\left\{(u^2)_{j-1/2}^{(i)} + \delta(u^2)_{j-1/2}^{(i)}\right\} + (p_3)_{j-1/2}^n\left\{(g)_{j-1/2}^{(i)} + \delta(g)_{j-1/2}^{(i)}\right\}$$

$$+\alpha_n(f_{j-1/2}^{(i)} + \delta f_{j-1/2}^{(i)})v_{j-1/2}^{n-1} - \alpha_n(v_{j-1/2}^{(i)} + \delta v_{j-1/2}^{(i)})f_{j-1/2}^{n-1} = R_{j-1/2}^{n-1}$$

$$\Rightarrow h_j^{-1}(v_j^{(i)} + \delta v_j^{(i)} - v_{j-1}^{(i)} - \delta v_{j-1}^{(i)}) + \left\{(p_1)_{j-1/2}^n + \alpha_n\right\}$$

$$\left\{(fv)_{j-1/2}^{(i)} + \frac{1}{2}(f_j^{(i)}\delta(v)_j^{(i)} + v_j^{(i)}\delta(f)_j^{(i)} + f_{j-1}^{(i)}\delta(v)_{j-1}^{(i)} + v_{j-1}^{(i)}\delta(f)_{j-1}^{(i)}\right\}$$

$$-\left\{(p_2)_{j-1/2}^n + \alpha_n\right\}\left\{(u^2)_{j-1/2}^{(i)} + u_j^{(i)}\delta(u)_j^{(i)} + u_{j-1}^{(i)}\delta(u)_{j-1}^{(i)}\right\}$$

$$+(p_3)_{j-1/2}^n\left\{(g)_{j-1/2}^{(i)} + \frac{1}{2}(\delta(g)_j^{(i)} + \delta(g)_{j-1}^{(i)})\right\}$$

$$+\alpha_n\left\{v_{j-1/2}^{n-1}(f_{j-1/2}^{(i)} + \frac{1}{2}(\delta f_j^{(i)} + \delta f_{j-1}^{(i)}) - (v_{j-1/2}^{(i)} + \frac{1}{2}(\delta v_j^{(i)} + \delta v_{j-1}^{(i)})f_{j-1/2}^{n-1}\right\}$$

$$= R_{j-1/2}^{n-1}$$

$$\Rightarrow (s_1)_j\,\delta v_j^{(i)} + (s_2)_j\,\delta v_{j-1}^{(i)} + (s_3)_j\,\delta f_j^{(i)} + (s_4)_j\,\delta f_{j-1}^{(i)} + (s_5)_j\,\delta u_j^{(i)}$$

$$+(s_6)_j\,\delta u_{j-1}^{(i)} + (s_7)_j\,\delta g_j^{(i)} + (s_8)_j\,\delta g_{j-1}^{(i)} + (s_9)_j\,\delta p_j^{(i)} + (s_{10})_j\,\delta p_{j-1}^{(i)} \tag{A34}$$

$$= (r_2)_j$$

Where $(s_1)_j = h_j^{-1} + \dfrac{(p_1)_{j-1/2}^n + \alpha_n}{2} f_j^{(i)} - \dfrac{1}{2}\alpha_n f_{j-1/2}^{n-1}$ (A35)

$$(s_2)_j = -h_j^{-1} + \frac{(p_1)_{j-1/2}^n + \alpha_n}{2} f_{j-1}^{(i)} - \frac{1}{2}\alpha_n f_{j-1/2}^{n-1} \tag{A36}$$

$$(s_3)_j = \frac{(p_1)_{j-1/2}^n + \alpha_n}{2} v_j^{(i)} + \frac{1}{2}\alpha_n v_{j-1/2}^{n-1} \tag{A37}$$

$$(s_4)_j = \frac{(p_1)_{j-1/2}^n + \alpha_n}{2} v_{j-1}^{(i)} + \frac{1}{2}\alpha_n v_{j-1/2}^{n-1} \tag{A38}$$

$$(s_5)_j = -\frac{(p_2)_{j-1/2}^n + \alpha_n}{2} u_j^{(i)} \tag{A39}$$

$$(s_6)_j = -\frac{(p_2)_{j-1/2}^n + \alpha_n}{2} u_{j-1}^{(i)} \tag{A40}$$

$$(s_7)_j = \frac{(p_3)_{j-1/2}^n}{2} \tag{A41}$$

$$(s_8)_j = \frac{(p_3)_{j-1/2}^n}{2} \tag{A42}$$

$$(s_9)_j = 0 \tag{A43}$$

$$(s_{10})_j = 0 \tag{A44}$$

$$(r_2)_j = R_{j-1/2}^{n-1} - \left\{ h_j^{-1}(v_j^{(i)} - v_{j-1}^{(i)}) + ((p_1)_{j-1/2}^n + \alpha_n)(fv)_{j-1/2}^{(i)} \right\}$$
$$+((p_2)_{j-1/2}^n + \alpha_n)\ (u^2)_{j-1/2}^{(i)} - \alpha_n(f_{j-1/2}^{(i)} v_{j-1/2}^{n-1} - f_{j-1/2}^{n-1} v_{j-1/2}^{(i)}) \tag{A45}$$
$$-(p_3)_{j-1/2}^n g_{j-1/2}^{(i)}$$

Here the coefficients $(s_9)_j$ and $(s_{10})_j$, which are zero in this case, are included here for the generality.

Similarly by using the equations (A23) to (A27) we get the equation (A21) in the following form:

$$(t_1)_j \delta p_j^{(i)} + (t_2)_j \delta p_{j-1}^{(i)} + (t_3)_j \delta f_j^{(i)} + (t_4)_j \delta f_{j-1}^{(i)} + (t_5)_j \delta u_j^{(i)}$$
$$+ (t_6)_j \delta u_{j-1}^{(i)} + (t_7)_j \delta g_j^{(i)} + (t_8)_j \delta g_{j-1}^{(i)} + (t_9)_j \delta v_j^{(i)} + (t_{10})_j \delta v_{j-1}^{(i)} \tag{A46}$$
$$= (r_3)_j$$

Where

$$(t_1)_j = \frac{1}{P_r}\left(1 + \frac{4}{3}p_4\right)h_j^{-1} + \frac{(p_1)_{j-1/2}^n + \alpha_n}{2} f_j^{(i)} - \frac{1}{2}\alpha_n f_{j-1/2}^{n-1} + \frac{4}{P_r}(p_4)_{j-1/2}^n \left(g^2 p\right)_j^i \tag{A47}$$

$$(t_2)_j = -\frac{1}{P_r}\left(1+\frac{4}{3}p_4\right)h_j^{-1} + \frac{(p_1)_{j-1/2}^n + \alpha_n}{2} f_{j-1}^{(i)} - \frac{1}{2}\alpha_n f_{j-1/2}^{n-1} + \frac{4}{p_r}(p_4)_{j-1/2}^n \left(g^2 p\right)_{j-1}^i \quad \text{(A48)}$$

$$(t_3)_j = \frac{(p_1)_{j-1/2}^n + \alpha_n}{2} + \frac{1}{2}\alpha_n p_{j-1/2}^{n-1} \quad \text{(A49)}$$

$$(t_4)_j = \frac{(p_1)_{j-1/2}^n + \alpha_n}{2} p_{j-1}^{(i)} + \frac{1}{2}\alpha_n p_{j-1/2}^{n-1} \quad \text{(A50)}$$

$$(t_5)_j = \frac{4}{p_r}(p_4)_{j-1/2}^n (gp^2)_j^i - \frac{1}{2}\alpha_n u_{j-1/2}^{n-1} - \frac{1}{2}\alpha_n u_j^i \quad \text{(A51)}$$

$$(t_6)_j = \frac{4}{p_r}(p_4)_{j-1/2}^n (gp^2)_{j-1}^{(i)} - \frac{1}{2}\alpha_n u_{j-1/2}^{n-1} - \frac{1}{2}\alpha_n u_{j-1}^{(i)} \quad \text{(A52)}$$

$$(t_7)_j = \frac{\alpha_n}{2} g_{j-1/2}^{n-1} - \frac{1}{2}\alpha_n g_j^{(i)} \quad \text{(A53)}$$

$$(t_8)_j = \frac{\alpha_n}{2} g_{j-1/2}^{n-1} - \frac{1}{2}\alpha_n g_{j-1}^{(i)} \quad \text{(A54)}$$

$$(t_9)_j = 0 \quad \text{(A55)}$$

$$(t_{10})_j = 0 \quad \text{(A56)}$$

$$(r_3)_j = T_{j-1/2}^{n-1} - \frac{1}{P_r}\left(1+\frac{4}{3}p_4\right) h_j^{-1}\left(p_j^{(i)} - p_{j-1}^{(i)}\right) - \frac{(p_1)_{j-1/2}^n + \alpha_n}{2}(fp)_{j-1/2}^{(i)}$$

$$-\frac{4}{p_r}(p_4)_{j-1/2}^n (gp^2)_{j-1/2}^{(i)} - \alpha_n\left(u_{j-1/2}^{(i)} g_{j-1/2}^{n-1} - u_{j-1/2}^{n-1} g_{j-1/2}^{(i)} - (ug)_{j-1/2}^{(i)}\right) \quad \text{(A57)}$$

$$+ \alpha_n\left(p_{j-1/2}^{(i)} f_{j-1/2}^{n-1} - p_{j-1/2}^{n-1} f_{j-1/2}^{(i)}\right)$$

The boundary conditions (A22) become

$$\delta f_0^n = 0,\ \delta u_0^n = 0,\ \delta p_0^n = 1$$
$$\delta u_J^n = 0,\ \delta g_J^n = 0 \quad \text{(A58)}$$

Which just express the requirement for the boundary conditions to remain during the iteration process.

References

Cebeci T.and Bradshaw P., Physical and Computational Aspects of Convective Heat Transfer, Springer, New York (1984)

Clarke J.F. and Riley N., 'Natural convection induced in a gas by the presence of a hot porous horizontal surface', *Q. J. Mech. Appl. Math.*, Vol. 28, pp. 373–396, (1975).

Clarke J.F. and Riley N., 'Free convection and the burning of a horizontal fuel surface', J. Fluid Mech.. Vol.74, pp. 415–431, (1976).

Cogley A.C., Vincenti W.G. and Giles S.E., 'Differential approximation for radiation transfer in a nongray near equilibrium', *AIAA Journal* , Vol.6 , pp. 551–553, (1968).

Hossain, M.A. and Ahmad, M. , 'MHD forced and free convection boundary layer flow near the leading edge', *Int. J Heat Mass Transfer,* Vol.33, No. 3, pp. 571-575, (1990).

Hossain, M .A., 'Viscous and joule heating effects on MHD-free convection flow with variable plate temperature', *Int. J Heat Mass Transfer.*, Vol.35, No.12, pp. 3485-3487, (1992).

Hossain M. A. and Takhar H. S, 'Radiation effect on mixed convection along a vertical plate with uniform surface temperature', *Heat and Mass Transfer,* Vol. 31, pp. 243-248, (1996).

Hossain. M.A., Alam, K.C.A. and Rees, D.A.S., 'MHD forced and free convection boundary layer flow along a vertical porous plate', *Applied Mechanics and Engineering*, Vol.2, No. 1, pp. 33-51, (1997).

Hossain, M. A. and Alim, M. A., Natural convection-radiation interaction on boundary layer flow along a Thin cylinder, *J Heat and Mass Transfer*, Vol. 32, pp. 515-520, (1997).

Hossain, M .A., Das, S. K. and Pop, I., 'Heat transfer response of MHD free convection flow along a vertical plate to surface temperature oscillation', *Int.J. Non- Linea Mechanics,* Vol. 33, No. 3, pp. 41-553. (1998).

Huang, M.J. and Chen, C.K., 'Laminar free convection from a sphere with blowing and suction', *J. Heat Transfer*, Vol. 109, pp. 529-532, (1987).

Keller H.B., 'Numerical methods in boundary layer theory, Annual Rev. Fluid Mechanics', Vol. 10, pp. 417-433, (1978).

Lin H.T. and Yu W.S., 'Free convection on a horizontal plate with blowing and suction, J. Heat Trans.'. *Trans. ASME* , Vol. 110, pp. 793–796, (1988).

Merkin, J.H. and Mahmood, T., 'On the free convection boundary layer on a vertical plate with prescribed surface heat flux', *J. Engg. Math*, Vol. 24, pp. 95-107, (1990).

Merkin,J.H. and Pop,I. 'Conjugate free convection on a vertical surface'. *Int. J Heat Mass Transfer*, Vol. 39, pp. 7, 1527-1534, (1982).

Miyamoto, M., Sumikawa, J., Akiyoshi , T. and Nakamura,T., 'Effects of axial heat conduction in a vertical flat plate on free convection heat transfer', *Int. J Heat Mass Transfer*, Vol. 23, pp. 1545-1553, (1980).

Nazar, R., Amin, N. and Pop, I., 'Free convection boundary layer flow on a horizontal circular cylinder with constant heat flux in a micropolar fluid', *Int Comm. Heat Mass Transfer*, Vol. 7. No. 2, pp. 409-431, (2002a).

Nazar, R., Amin, N., Grosan, T. and Pop, I., 'Free convection boundary layer on an isothermal sphere in a micropolar fluid', *Int. Comm. Heat Mass Transfer*, Vo. 29, No.3, pp. 377-386, (2002b).

Özisik, M. N., Radiative Transfer and Interactions with Conduction and Convection, Wiley, New York, (1973).

Pozzi. A. and Lupo, M. 'The coupling of conduction with laminar natural convection along a flat plate', *Int. J Heat Mass Transfer*, Vol. 31, No.8, pp. 1807-1814, (1988).

Siegel, R., Howell, J. R., Thermal Radiation Heat Transfer. NY: McGraw-Hill (1972)

Soundalgekar. V. M., Takhar H. S. and Vighnesam N.V., 'The combined free and forced convection flow past a semi-infinite vertical plate with variable surface temperature', *Nuclear Engineering and Design* , Vol.110, pp. 95-98, (1960).

Taher, M. A. and Molla. M. M., 'Natural convection boundary layer flow on a sphere in presence of heat generation', *proceeding of the 5th International conference on Mechanical Engineering and 10th annual paper meet*, Dhaka. pp. 223-228, (2005).

Vedhanayagam M., Altenkirch R. A. and Eichhorn, R., 'A transformation of the boundary layer equations for free convection past a vertical flat plate with arbitrary blowing and wall temperature variations'. *Int J. Heat Mass Tran.*. Vol. 23, pp. 1286-1288, (1980).

Yao, L.S., 'Natural convection along a vertical wavy surface'. *ASME J. Heat Transfer*, Vol. 105, pp. 465-468, (1983).